（明治大学理工学部研究報告 第14号（70）・1996年3月）

Ⅶ-2 On the Origin of a Split EPR Signal from a Modified S_3'-State of Ca^{2+}-Depleted Photosystem II in Plants

楠　正美*

Masami KUSUNOKI*

（1996年1月19日受理）

Abstract

An effective spin hamiltonian that can properly describe the isotropic exchange and magnetic dipolar interactions between a Mn-tetramer with total spin $S_1=1/2$ and its ligand radical with spin $S_2=1/2$, i.e., $J_{12}\mathbf{S}_1 \cdot \mathbf{S}_2$ and $\mathbf{S}_1 \cdot \mathbf{D}_{12} \cdot \mathbf{S}_2$, respectively, has been quantum-mechanically derived to elucidate the origin of a new type of EPR signals from the modified-S_3 (S_3') state of Ca^{2+}-depleted photosysten II (PS II) membranes. This signal, called "S_3' signal", is centered at g=2.004 and notably consists of a main doublet component having a near-symmetric lineshape with the linewidth of 100-200 G and a secondary wing component asymmetrically extending over ≈ 910 G without any hyperfine structure. From results of computer simulation of the S_3' signal, combined with the pulsed EPR data, it follows: (1) the Mn_4-radical complexes in the S_3' state must be highly inhomogeneous; (2) the majority (≈ 77 %) would be EPR-silent possibly because of no detectable magnetic moment due to $J_{12} \gg k_BT$ (temperature), and (3) the minority would exhibit an EPR signal mainly contributing to the doublet (≈ 15 %) or wing (≈ 8 %) component in the S_3' signal according as $|J_{12}| \approx$ 100-200 G or $|J_{12}| \gg$ 100-200 G (together with an additional condition, $J_{12} < k_BT$, when $J_{12} > 0$), respectively, indicating (4) the radical could be neither an oxidized histidine [Boussac et al. (1990) Nature 347,303-306] nor tyrosine Y_Z^+[Hallahan et al.(1992) Biochemistry 31, 4562-4573] but some bridging ligand; (5) the doublet component can arise only from the weakly-coupled Mn_4-radical complexes satisfying the conditions for a small near-isotropic interaction ($|J_{12}| \approx$ 100-200 G $\gg |\mathbf{D}_{12}|$) and having the tetrameric effective Mn-spins with appreciable hyperfine coupling constants, indicating (6) the radical must form the third asymmetrically-bridging ligand between di(μ-oxo) bridged Mn_a(III) and Mn_b(IV) ions on the opposite side of the other pair of Mn_c(IV) and Mn_d(IV) ions in an asymmetric Mn-tetramer whose spin state is approximately given by $\psi_1(1/2M)=\cos\theta_0|S_{ab}(1/2)S_{cd}(0)S_1(1/2)M\rangle + \sin\theta_0|S_{ab}(1/2)S_{cd}(1)S_1(1/2)M\rangle$ with $\theta_0 \approx -62° \sim -65°$, and (7) the radical takes the g-value of ca. 2.011, which is much larger than the free electron g-value (g_e=2.0023), nearly equal to that of $OH\cdot$(≈2.011) and slightly less than that of $O_2^{-\cdot}$ (≈2.015), indicative of an oxygen-rich moiety rather than an aromatic amino acid. These findings, together with the reported stoichiometry of protons released during the normal S-state cycle, evidently suggest that the radical as the primary water-oxidation product would be most likely $(HO^-)(HO^\cdot)$ or $(HOOH^\cdot)^-$, being bound on the catalytic microsurface of the di(μ-oxo)Mn_2(III,IV) subunit in both the normal and the modified S_3 states.

Key Words: Photosystem II / Water Oxidase / Electron Paramagnetic Resonance / Manganese Cluster / Ca^{2+} / Oxygen Evolution

1. Introduction

Manganese and calcium are vital cofactors for the photosynthetic O_2 evolution that takes place as a result of light-driven water oxidation in plant photosystem II (PSII). The O_2-evolving complex (OEC)

＊　明治大学理工学部物理学科

phenomenologically cycles through five redox states, denoted as S_i (i=0, 1,, 4), depending upon the number of electrons abstracted from the reaction center $P680^+$: only S_1 is stable in the dark and S_4 represents a transient state just before emitting O_2 during the $S_3 \rightarrow (S_4) \rightarrow S_0$ transition[1] The stoichiometry of four protons released from the enzyme-substrate (water) complex during an S-state cycle is thought to be most likely 1:0:1:2 on the $S_0 \rightarrow S_1$: $S_1 \rightarrow S_2$: $S_2 \rightarrow S_3$: $S_3 \rightarrow (S_4) \rightarrow S_0$ transitions, although the other possibility can not be ruled out. The active site of this enzyme has been recently evidenced to contain four manganese and one calcium ions forming an exchange-coupled Mn-tetramer (Mn_4)[2,3], with the Ca^{2+} ion being bound nearby[4]. The molecular and submolecular structure of the Mn_4 complex and whether it accumulates all four oxidizing equivalents before water oxidation in response to the four successive charge-separations, has been a subject of vigorous debate (see the most recent comprehensive reviews[5]) .

Since a paramagnetic ^{55}Mn ion has a nuclear spin I=5/2 strongly interacting with the electronic spin, the low-temperature EPR spectroscopy can provide a unique and direct method to investigate not only the molecular structure of the Mn cluster but also the roles of four Mn ions in storing the oxidizing equivalents and serving as the catalytic site of water decomposition. Below 35 K, Dismukes and Siderer[6] first discovered a broad EPR signal, named "multiline signal" because of its containing 18-20 hyperfine lines spaced by 85-90 G around g=2.0 at X-band frequency, and ascribed it to an S=1/2 Mn-dimer or Mn-tetramer in the S_2 state. It is generally agreed that the multiline signal arises from an S=1/2 ground state of a tetranuclear Mn_4(III,III,III,IV) or Mn_4(III,IV,IV,IV) cluster[5]. When the PS II membranes are depleted of one Ca^{2+} ion per PS II by low-pH treatment and then are illuminated, an altered multiline EPR signal with ≈ 26 hyperfine lines spaced by 55-65 G, which is rather stable in darkness, appears, indicating that the S_2 state Mn-cluster can persist in a modified form in the absence of the Ca^{2+} cofactor[7-9] . A variety of altered multiline signals were reported: e.g. treatment with NH_3 yielded a signal having more lines (21-22 vs 18-20) and smaller hyperfine splittings (67.5 G vs 87.5 G) than the unmodified signal[10]. Such remarkable sensitivity on sample treatment was attributed to a sensitivity of the effective hyperfine coupling constants on small change of the exchange interactions within the cluster [2,11]. The proper quantum theory[2] revealed that the most probable cluster configuration responsible for the multiline signal would be a tetranuclear Mn_4(III,IV,IV,IV) complex involving a strong antiferromagnetic exchange interaction between Mn_a(III) and Mn_b(IV) ions ($J_{ab}S_a \cdot S_b$; J_{ab}= 200-300 cm^{-1}) and the other intermediate or weak ones ($J_{ij}S_i \cdot S_j$; $|J_{ij}| \ll J_{ab}$ for ij≠ab).This assignment to the higher-valent state agrees with recent refined analyses of the Mn pre-K-edge XANES(X-ray Absorption Near Edge Structure) [12] and principal XANES [4] spectra. The Requirement of only one 2.7 Å Mn-Mn interaction present in the tetramer, however, seems to be contradictory to the EXAFS (Extended X-ray Absorption Fine Structure) data[4].

A second broad EPR signal was soon found to appear at around g=4.1-4.2 in a different S_2 state [13,14]. This "g=4" signal was found to be modified by treatment with NH_4Cl [15], but to disappear by Ca^{2+}-depletion. The NH_3-modified g=4 signals from oriented PSII membranes, which exhibit at least 16 partially resolved hyperfine lines spaced by 36 G [15], were well simulated based on the assumption that it would arise from a middle Kramers doublet of the lowest S=5/2 state of a Mn_4(III,IV,IV,IV) tetramer different from that mentioned above[11], substantiating a recent proposal[16]. Consistent with this theory, a strong experimental evidence for the heterogeneity of paramagnetic species has been provided by interesting correlation between the multiline and g=4 signals [17,18].

Any broad EPR signal due to S_3 has been sought in vain. Nevertheless, a new EPR signal arising from a formal S_3 state has been reported in Ca^{2+}-depleted[7-9], NH_3-treated[19] and acetate-treated[20] PSII. This S_3' signal has the following characteristics: (i) It is centered at g=2.004; (ii) the spectrum has a complex structure mainly consisting of a narrow doublet with a near-symmetric linewidth and a 100-240 G linewidth, which sensitively depends upon sample treatments, and a pair of broad wings asymmetrically extending over the range 2950-3860 G at an X-band frequency[19]; (iii) the intensity obeys the Curie law on the temperature dependence[21]; and (iv) its integrated signal area is only 23% of that of the S_2 multiline signal [22].

Boussac et al.[23] explained the doublet component of the S_3' signal by assuming that the $S_2' \rightarrow S_3'$ transition occurring in Ca^{2+}-depleted PSII corresponds to the oxidation of histidine capable of magnetically interacting with the $S_1=1/2$ Mn cluster in the S_2' state. This explanation is mainly based on the observations that the optical absorption difference spectrum between S_2 and S_3 is similar to an absorption spectrum of [His-OH]· radical[24], and that the XANES spectra observed in the S_2 and S_3 (65%S_3, 35%S_2) states[25] are indistinguishable. An alternative origin of the S_3' signal was recently proposed by Hallahan et al.[26] to be a trapped tyrosine $Y_z^{+\cdot}$ instead of His·, although the experimental data were pointed out to be artifactual due to the use of saturating microwave powers [27]. These models, however, contradict recent measurements of laser-flash induced XANES spectra from both the control [28] and the Ca^{2+}-depleted [29] PS II, indicating that a Mn(III) or Mn(IV) ion or its direct ligand was oxidized upon the $S_2(S_2') \rightarrow S_3(S_3')$ transition. Furthermore, any model of photooxidation of a particular protein residue has a serious difficulty in explaining why the normal S_3 state can not show such a characteristic EPR signal centered at $g \approx 2$.

In this paper, it will be shown that the S_3' signal can be regarded as the first experimental evidence of a primary water oxidation process taking place upon the $S_2 \rightarrow S_3$ transition. We first derive an effective spin hamiltonian for a paramagnetic Mn_4-radical complex which is assumed to consist of coupled half spins of the Mn_4(III,IV,IV,IV)-tetramer ($S_1=1/2$) and the ligand radical ($S_2=1/2$). Next, we determine the singlet-triplet energy levels and the EPR transition probabilities, by invoking the second order perturbation theory. Next, we examine what model Mn_4-radical complexes can exhibit a 90-240 Gauss-wide doublet spectrum indicative of a very weak magnetic interaction between the $\mathbf{S}_1$ and $\mathbf{S}_2$ spins, by adopting the most probable model complex whose spin state vector can be expanded as described in the above abstract. As for this model complex, we investigate some critical roles of the phase angle θ_0 on the S_3' EPR signal, involving three important effects of (i) a "magic phase angle" where a pair of Mn spins effectvely vanish, (ii) the effective exchange interaction J_{12} and (iii) the magnetic dipolar interaction $\mathbf{D}_{12}$ between $\mathbf{S}_1$ and $\mathbf{S}_2$, and simulate a reported S_3' signal [23] together with predictions of the orientation dependence and the H/D isotope effect, by assuming an inhomogeneous J_{12}-distribution. Finally, we discuss and summarize some reasons why the radical may be exclusively assigned to $(HOOH\cdot)^-$, which is predicted to be bound as the third bridging ligand between di(μ-oxo) bridged Mn(III) and Mn(IV) ions.

2. The Spin Hamiltonians

In both the S_3 and the S_3' states, the paramagnetic center is assumed to consist of four exchange-coupled Mn spins in the catalytic Mn tetramer ($\mathbf{S}_i$, i=a, b, c, d) and one radical spin nearby ($\mathbf{S}_2$). Its total spin hamiltonian in a magnetic field $\mathbf{B}$ can be written as

$$H_{tot} = H_{Mn} + H_R + H_{int}, \tag{1}$$

$$\begin{aligned} H_{Mn} = &\sum_{i>j} J_{ij} S_i \cdot S_j + \sum_{i=a}^{d} \beta S_i \cdot a_i \cdot I_i \\ &+ \sum_{i>j} S_i \cdot D_{ij} \cdot S_j + \sum_{i=a}^{d} S_i \cdot D_i \cdot S_i, \end{aligned} \tag{2}$$

$$H_R = \beta S_2 \cdot g_2 \cdot B + \sum_k S_2 \cdot a_k \cdot I_k, \tag{3}$$

$$H_{int} = \sum_{i=a}^{d} (J_{i2} S_i \cdot S_2 + S_i \cdot D_{i2} \cdot S_2), \tag{4}$$

where the various terms represent the isotropic exchange ($J_{ij}\mathbf{S}_i \cdot \mathbf{S}_j$), electronic Zeeman ($\beta \mathbf{S}_i \cdot \mathbf{g}_i \cdot \mathbf{B}$), nuclear hyperfine ($\mathbf{S}_i \cdot \mathbf{a}_i \cdot \mathbf{I}_i$), crystal field ($\mathbf{S}_i \cdot \mathbf{D}_i \cdot \mathbf{S}_i$) and magnetic dipolar plus anisotropic exchange ($\mathbf{S}_i \cdot \mathbf{D}_{ij} \cdot \mathbf{S}_j$) interactions. The constants involved here have all their usual meanings. In the expression of H_{Mn}, we imply that the J_{ij} values in the S_3-state would be different from those in the S_2-state owing to a further distortion of the Mn tetramer upon the $S_2 \rightarrow S_3$ transition. However, this difference may not be large enough to destabilize the singlet ground state, because (1) the doublet component also obeys the Curie law[21] and (2) the spin-lattice relaxation times of the Y_D^+ EPR signal due to the paramagnetic Mn spins were essentially the same in the S_2 and S_3 states[30]. Hence, the spin state vector of the Mn-tetramer in S_3 is in the zeroth approximation given by the S_1=1/2 ground state of the exchange hamiltonian in H_{Mn} and can be expanded as

$$\psi_1(\frac{1}{2}M) = \cos\theta_0 |S_{ab}(\frac{1}{2})S_{cd}(0)S_1(\frac{1}{2})M\rangle + \sin\theta_0 |S_{ab}(\frac{1}{2})S_{cd}(1)S_1(\frac{1}{2})M\rangle, \quad (5)$$

with

$$\tan 2\theta_0 = -\frac{3p_{10}J_-}{J_{cd} - J_+}, \quad (6)$$

under the ground state condition $J_-\tan\theta_0 < 0$, where $J_\pm \equiv J_{ac} \pm J_{ad} - (J_{bc} \pm J_{bd})/2$ and p_{10}={√(5/3) for Model I: Mn_4(III,IV,IV,IV); √(8/3) for Model II: Mn_4(III,IV,III,III)}[2]. Namely, the S_3-state Mn cluster can be regarded as a singlet-triplet mixing system consisting of the Mn-tetramer with spin $S_1=|S_a+S_b+S_c+S_d|=1/2$ and a radical with spin S_2=1/2. Then, the effective spin hamiltonian can be readily derived by a vector projection method based on the Wigner-Eckart theorem [31]:

$$H^* = \{\beta \mathbf{S_1}\cdot\mathbf{g_1}\cdot\mathbf{B} + \mathbf{S_1}\cdot\sum_{i=a}^{d} P_i\mathbf{a_i}\cdot\mathbf{I_i}\} + \{\beta\mathbf{S_2}\cdot\mathbf{g_2}\cdot\mathbf{B} + \mathbf{S_2}\cdot\sum_k \mathbf{a_k}\cdot\mathbf{I_k}\} + J_{12}\mathbf{S_1}\cdot\mathbf{S_2} + \mathbf{S_1}\cdot\mathbf{D_{12}}\cdot\mathbf{S_2}, \quad (7)$$

with

$$\mathbf{g_1} = \sum_{i=a}^{d} P_i \mathbf{g_i}, \quad (8)$$

$$P_i = \langle\psi_1(\frac{1}{2}M)|\mathcal{P}_i|\psi_1(\frac{1}{2}M)\rangle; \mathcal{P}_i = \frac{\mathbf{S_i}\cdot\mathbf{S_1}}{S_1(S_1+1)}, \quad (9)$$

$$J_{12} = \sum_{i=a}^{d} P_i J_{i2}, \quad (10)$$

$$\mathbf{D_{12}} = \sum_{i=a}^{d} P_i \mathbf{D_{i2}}, \quad (11)$$

Here, it should be noted that the zero-field splitting terms other than $\mathbf{D_{i2}}$ (i=a-d) exactly vanish because of $S_1=S_2=1/2 < 1$. Thus, we find that both the isotropic (J_{12}) and the anisotropic ($\mathbf{D_{12}}$) interactions between two half spins strongly depend on the radical binding site and also on the conformational state of the Mn tetramer, via $\{P_i, J_{i2}, \mathbf{D_{i2}}\}$.

The essential role of the off-diagonal matrix elements of projection operators $\{\mathcal{P}i\}$ on the effective spin hamiltonian was first demonstrated in ref 2. In Appendix A, we give general formulae to analytically calculate the matrix elements of $\{\mathcal{P}i$; i=a-d$\}$. Applying them to the present system (S_a=2, $S_b=S_c=S_d$=3/2) yields

$$P_a(\theta_0) = -2P_b(\theta_0) = \frac{2}{3}(1+2\cos 2\theta_0),$$
$$P_c(\theta_0) = \frac{1}{3}(1-\cos 2\theta_0) + p_{10}\sin 2\theta_0, \quad (12a\text{-}d)$$
$$P_d(\theta_0) = \frac{1}{3}(1-\cos 2\theta_0) - p_{10}\sin 2\theta_0.$$

The $P_i(\theta_0)$ vs θ_0 relations (i=a-d), which are plotted in Fig.1, significantly display that both $P_a(\theta_0)$ and $P_b(\theta_0)$, hence the effective spins of Mn_a(III) and Mn_b(IV) ions, vanish at $\theta_0 = \pm 60°$, and $P_c(\theta_0)$ and $P_d(\theta_0)$, hence the effective spins of Mn_c(IV) and Mn_d(IV) ions, do at θ_0=0°. Since a radical directly bound to the ith Mn ion is usually considered to introduce strong interactions between them, J_{i2} and $\mathbf{D_{i2}}$, the possibility that the effective interactions, $J_{i2}P_i(\theta_0)$ and $\mathbf{D_{i2}}P_i(\theta_0)$, could almost diminish at some conformational substate of the Mn cluster is exactly consistent with the fact that the normal S_3-state does not show any EPR signal, while some modified S_3'-state does the narrow doublet EPR signal with the separation of 100-200 G, indicative of a dramatic decrease of the effective interactions. This decrease is expected to be of 2-3 orders of magnitude in the present hypothesis. Namely, a reason why the normal S_3-state is EPR-silent may be that it could be in the singlet ground state due to the antiferromagnetic exchange interaction J_{12} much larger than kT. For the S_3' state to exhibit such a narrow doublet signal, $\mathbf{D_{12}}$ must also dramatically decrease in the order of magnitude at least to the same level as J_{12} . Since the dipolar interaction has the long range nature, this condition imposes some useful restrictions to the possible models of Mn cluster, as will be shown later.

Usually, $\mathbf{D}_{i2}$ consists of two contributions from the dipolar and pseudo-dipolar (anisotropic exchange) interactions between the ith Mn and radical spins. The former may be treated in the point-dipole approximation and takes the magnitude of the order of $6B_0/r_{i2}^3$ at separation r_{i2}: the typical value is 0.3 cm^{-1}($\approx$ 3210 G) at r_{i2}=2 Å, because B_0=0.4330 cm^{-1}(=4637 G). On the other hand, the latter is known to arise from a combined effect of the spin-orbit coupling $H_{LSi} = \lambda_i \mathbf{L}_i \cdot \mathbf{S}_i$ for the ith Mn ion and the anisotropic exchange coupling between the Mn and radical spins. A simple formula, $(g_i - 2)^2 J_{i2}^*$,[32] has been widely adopted to make the order-of-magnitude estimation. Since g-values of Mn spins have been observed to be, typically, $\{g_\perp=1.993, g_\parallel=1.963\}$ for Mn(III) ion [33] and $\{g_\perp=2.000, g_\parallel=1.995\}$ for Mn(IV) ion [34], if this formula is appropriate, the pseudo-dipolar term might be neglected in the case of Mn(IV) ion, but not in the case of Mn(III) ion, because in which D_{pd} could amount to 0.13 cm^{-1} at $g_i=g_\parallel$=1.963 by assuming an overestimated value of $J_{i2}^* \approx 100$ cm^{-1} (see Section 3). However, we have shown in Appendix B that this formula overestimates the D_{pd} by a factor 8^2x5/2=160, and hence this pseudo-dipolar term may be neglected in the present problem. Thus, one may assume that $\mathbf{D}_{12}$ takes the form:

$$\mathbf{D}_{12} = \beta^2 \sum_{i=a}^{d} \left[\frac{\mathbf{g}_i^t \mathbf{g}_2}{r_{i2}^3} - \frac{3(\mathbf{g}_i^t \mathbf{r}_{i2})(\mathbf{r}_{i2}\mathbf{g}_2)}{r_{i2}^5}\right] P_i(\theta_0), \qquad (13)$$

where subscript t represents the matrix transpose operation, and $\mathbf{r}_{i2}$ is the coordinate vector of the ith Mn ion relative to the center of the radical spin. Let us put the principal axes of tensor $\mathbf{D}_{12}$ to be X, Y and Z and assume for simplicity all the g_i-tensors in eq 13 to be isotropic. Then, in the XYZ coordinate system, we have

$$\mathbf{D}_{12} = \begin{bmatrix} E_{12} - D_{12}/3 & 0 & 0 \\ 0 & -E_{12} - D_{12}/3 & 0 \\ 0 & 0 & 2D_{12}/3 \end{bmatrix}, \qquad (14)$$

with

$$D_{12}(\theta_0) \equiv \frac{3}{2} D_{12}^{ZZ} \approx \frac{3}{2} g_2 \beta^2 \sum_{i=a}^{d} \frac{g_i P_i(\theta_0)}{r_{i2}^3}(1 - 3\cos^2\theta_{i2}), \qquad (15)$$

and

$$D_{12}(\theta_0) \equiv \frac{1}{2}(D_{12}^{XX} - D_{12}^{YY}) \approx -\frac{3}{2} g_2 \beta^2 \sum_{i=a}^{d} \frac{g_i P_i(\theta_0)}{r_{i2}^3} \sin^2\theta_{i2} \cos 2\phi_{i2}, \qquad (16)$$

where a set of polar angles $\{\theta_{i2}, \phi_{i2}; i=a\text{-}d\}$ must satisfy the following relations:

$$D_{12}^{XY} = D_{12}^{XY} \approx \frac{1}{2} g_2 \beta^2 \sum_{i=a}^{d} \frac{g_i P_i(\theta_0)}{r_{i2}^3} \sin 2\theta_{i2} \sin 2\phi_{i2} = 0, \qquad (17a)$$

$$D_{12}^{XY} = D_{12}^{ZY} \approx \frac{1}{2} g_2 \beta^2 \sum_{i=a}^{d} \frac{g_i P_i(\theta_0)}{r_{i2}^3} \sin 2\theta_{i2} \sin \phi_{i2} = 0, \qquad (17b)$$

and

$$D_{12}^{XZ} = D_{12}^{ZX} \approx \frac{1}{2} g_2 \beta^2 \sum_{i=a}^{d} \frac{g_i P_i(\theta_0)}{r_{i2}^3} \sin 2\theta_{i2} \cos \phi_{i2} = 0, \qquad (17c)$$

3. Energy Levels and Transition Probabilities

In order to simplify the present eigen value-eigen vector problem for the effective spin hamiltonian H^* of eq 7, which contains a number of non-collinear $\mathbf{g}_1$, $\mathbf{g}_2$, $\mathbf{a}_i$ (i=a-d), $\mathbf{a}_k$ (k=e,..) and $\mathbf{D}_{12}$ tensors, we assume that the anisotropy of the $\mathbf{D}_{12}$ tensor predominates over the others which will be neglected except their possible contributions to the Gaussian line broadening. When a high magnetic field $\mathbf{B}$ is applied in a direction with polar angles (θ, ϕ) in the XYZ coordinate system, it provides the best quantization axis ("z-axis") not only for the electronic spins $\mathbf{S}_1$ and $\mathbf{S}_2$, yielding the respective Zeeman energy terms, $\beta g_1 B S_{1z}$ and $\beta g_2 B S_{2z}$, but also for the nuclear spins $\mathbf{I}_i$ (i=a-d) and $\mathbf{I}_k$ (k=e,...), doing the respective hyperfine splitting terms dominated by

$\sum_{i=a}^{d} P_i(\theta_0) a_i S_{iz} I_{iz}$ and $\sum_{k=e} a_k S_{kz} I_{kz}$.

This new xyz-coordinate system corresponds to the laboratory frame, in which the principal X, Y, and Z axes have the direction cosines forming a unitary transformation matrix U: a convenient choice is

$$U = \begin{bmatrix} \sin\phi, & \cos\theta\sin\theta, & \sin\theta\cos\theta \\ -\cos\theta, & \cos\theta\sin\phi, & \sin\theta\sin\phi \\ 0, & -\sin\theta, & \cos\theta \end{bmatrix}$$

(note that the x-axis lies in the principal XY-plane). Then, the transformed matrix $U^t \mathbf{D}_{12} U$ can be readily calculated, yielding a dipolar interaction hamiltonian

$$H_D = A(\theta,\phi)\{S_{1z}S_{2z} - \frac{1}{4}(S_{1+}S_{2-} + S_{1-}S_{2+})\} + H_D', \tag{18}$$

with

$$A(\theta,\phi) = D_{12}(\cos^2\theta - \frac{1}{3}) + E_{12}\sin^2\theta\cos 2\phi, \tag{19}$$

and

$$\begin{aligned} H_D' &= E_{12}\sin\theta\sin 2\phi(S_{1x}S_{2z} + S_{1z}S_{2x}) \\ &+ \frac{1}{2}(E_{12}\cos 2\phi - D_{12})\sin 2\theta(S_{1y}S_{2z} + S_{1z}S_{2y}) \\ &- \frac{1}{4}[\{E_{12}\cos 2\phi(1+\cos^2\theta) + D_{12}\sin^2\theta \\ &+ 2iE_{12}\sin 2\phi\cos\theta\}S_{1+}S_{2+} + \text{h.c.}], \end{aligned} \tag{20}$$

where $S_{j\pm} \equiv S_{jx} \pm iS_{jy}$ (j=1,2) and h.c. stands for hermitian conjugate. In eq 18, the first term represents the important conservative motion of an electronic total spin ($\Delta M=0$), while the second (H_D') does a non-conservative one with $\Delta M=\pm1$ or ±2, which will be later found to be negligible. On the other hand, the motions of the nuclear spins are individually conservative, i.e. $\Delta m_{Ii}=0$ (i=a-d) and $\Delta m_{Ik}=0$ (k=e,..), in the first order approximation of each hyperfine coupling term. Thus, the energy levels designated by a set of nuclear spin quantum numbers, $\{m_{Ii}=-5/2, \cdots, 5/2$ for $^{55}Mn\}$ and $\{m_{Ik}=-I_k, \cdots, I_k$ for nuclear spins in the radical$\}$, can be obtained by diagonalizing the zeroth order spin hamiltonian:

$$\begin{aligned} H_0^*(\{m_I\}) &= [\beta g_1 B + 2h_1(\{m_{Ii}\})]S_{1z} \\ &+ [\beta g_2 B + 2h_2(\{m_{Ik}\})]S_{2z} \\ &+ \{J_{12} + A(\theta,\phi)\}S_{1z}S_{2z} \\ &+ \frac{1}{4}\{2J_{12} - A(\theta,\phi)\}(S_{1+}S_{2-} + S_{1-}S_{2+}), \end{aligned} \tag{21}$$

with

$$h_1(\{m_{Ii}\}) = \frac{1}{2}\sum_{i=a}^{d} P_i a_i m_{Ii}, \tag{22}$$

$$h_2(\{m_{Ik}\}) = \frac{1}{2}\sum_{k=e} a_i m_{Ik}. \tag{23}$$

The eigenvectors take the form

$$\begin{aligned} |\Phi_1\rangle &= \alpha(1)\beta(2), \\ |\Phi_2\rangle &= \cos\Theta\alpha(1)\beta(2) + \sin\Theta\beta(1)\alpha(1), \\ |\Phi_3\rangle &= -\sin\Theta\alpha(1)\beta(2) + \cos\Theta\beta(1)\alpha(2), \\ |\Phi_4\rangle &= \beta(1)\beta(2), \end{aligned} \tag{24a-d}$$

and the corresponding eigenvalues are given by

$$\begin{aligned} E_1 &= \beta B(g1+g2)/2 + h_1 + h_2 + (J_{12}+A)/4, \\ E_2 &= -(J_{12}+A)/4 + C, \\ E_3 &= -(J_{12}+A)/4 - C, \\ E_4 &= -\beta B(g1+g2)/2 - h_1 - h_2 + (J_{12}+A)/4, \end{aligned} \tag{25a-d}$$

with

$$\Theta = \mathrm{Tan}^{-1}[\frac{2C - \beta B(g_1 - g_2) - 2(h_1 - h_2)}{j_{12} - \frac{1}{2}A}], \tag{26}$$

$$C = \sqrt{\{\frac{1}{2}\beta B(g_1 - g_2) + h_1 - h_2\}^2 + \frac{1}{4}(J_{12} - \frac{A}{2})^2}. \tag{27}$$

When an oscillatory magnetic field $\mathbf{B}_\nu$ at frequency ν is applied along a direction perpendicular to $\mathbf{B}$, the perturbation hamiltonian to induce the transitions is given by

$$\begin{aligned} H'(t) = \frac{1}{2}B_\nu\beta[&(g_1S_{1+} + g_2S_{2+})e^{-2\pi i\nu t} \\ &+ (g_1S_{1-} + g_2S_{2-})e^{2\pi i\nu t}]. \end{aligned} \tag{28}$$

The selection rule $\Delta M=\pm1$ picks up four possible transitions: $3\rightarrow1$, $4\rightarrow2$, $2\rightarrow1$ and $4\rightarrow3$, with the relative intensities given by $(g_1\cos\Theta-g_2\sin\Theta)^2$, $(g_1\cos\Theta+g_2\sin\Theta)^2$, $(g_2\cos\Theta+g_1\sin\Theta)^2$ and $(g_2\cos\Theta-g_1\sin\Theta)^2$, respectively, and with the resonance magnetic fields:

$$B_{31} = B_+ - B_{int,+} - \sqrt{[(B_- + B_{int,-})^2 + B_{int,0}^2]},$$
$$B_{42} = B_+ + B_{int,+} - \sqrt{[(B_- - B_{int,-})^2 + B_{int,0}^2]},$$
$$B_{21} = B_+ - B_{int,+} + \sqrt{[(B_- + B_{int,-})^2 + B_{int,0}^2]},$$
$$B_{43} = B_+ + B_{int,+} + \sqrt{[(B_- - B_{int,-})^2 + B_{int,0}^2]}, \qquad (29a\text{-}d)$$

respectively, where

$$B_\pm = \frac{h\nu}{2\beta}\left(\frac{1}{g_1} \pm \frac{1}{g_2}\right) - \left(\frac{h_1}{\beta g_1} \pm \frac{h_2}{\beta g_2}\right), \qquad (30a/b)$$
$$B_{int,\pm} = \frac{g_1 \pm g_2}{4\beta g_1 g_2}(J_{12} + A), \qquad (31a/c)$$
$$B_{int,0} = \frac{1}{2\beta\sqrt{g_1 g_2}}\left(J_{12} - \frac{1}{2}A\right). \qquad (31b)$$

In this approximation, the EPR signal must be symmetric contrary to the observation showing a small asymmetry. One can attribute this asymmetry mainly to the off-diagonal components of the strong hyperfine couplings between manganese electronic and nuclear spins. In the second order perturbation theory, this effect appears as the shifts of energy levels:

$$\Delta E_1(\{m_{Ii}\}) \cong \sum_{i=a}^{d} \frac{(P_i a_i)^2}{4h\nu}\{I(I+1) - m_{Ii}(m_{Ii}+1)\},$$
$$\Delta E_2(\{m_{Ii}\}) = \cos 2\Theta \Delta E_1(\{m_{Ii}\}),$$
$$\Delta E_3(\{m_{Ii}\}) = \cos 2\Theta \Delta E_4(\{m_{Ii}\}),$$
$$\Delta E_4(\{m_{Ii}\}) \cong -\sum_{i=a}^{d} \frac{(P_i a_i)^2}{4h\nu}\{I(I+1) - m_{Ii}(m_{Ii}-1)\}, \qquad (32a\text{-}d)$$

which in turn lead to the shifts of resonance magnetic fields: $B_{ij} \rightarrow B_{ij} - (\Delta E_i - \Delta E_j)/2\beta$. Finally, we must check the effect of H_D' of eq 20 on orientation-dependent level shifts. In the case of axial symmetry ($E_{12}=0$), we have $\Delta E_1'=-\Delta E_4'= (D_{12}^2/32h\nu)(1+\cos^2\theta)\sin^2\theta$ and $\Delta E_2'=\Delta E_3'=0$ (all the energy denominators are approximated by $h\nu$): At $\theta=45°$, the shifts are estimated to be less than 1 G when $|D_{12}| < 300$ G at X-band frequency. Hence, we can safely neglect it.

It would be instructive to consider two limiting situations:

(i) *The weak coupling limit:* $J_{12} \rightarrow 0$, $A \rightarrow 0$

In this limit, the EPR absorptions by spins, S_1 and S_2, must be independent. In fact, with Θ defined by eq 26 using Tan^{-1} ($-\pi/2 \le \Theta \le \pi/2$), the four transitions become separable into two groups belonging to S_1 and S_2: e. g. in the case of $g_1=g_2$, the S_1 / S_2 groups are described by a couple of resonance fields: (B_{31}, B_{43}) / (B_{21}, B_{42}) with $\Theta=0$ for $h_1 > h_2$, and (B_{21}, B_{42}) / (B_{31}, B_{43}) with $\Theta=\pi/2$ or $-\pi/2$ (according as $J_{12}-A/2 >0$ or <0) for $h_1< h_2$, respectively.

(ii) *The strong exchange coupling limit:* $|J_{12}| >> |A|$, $|g_1-g_2|h\nu$, $|h_1|$, and $|h_2|$

In this limit, the spin system splits into singlet and triplet levels and the EPR-susceptible triplet levels become (1,2,4) with $\Theta=\pi/4$ or (1,3,4) with $\Theta=-\pi/4$ according as $J_{12} > 0$ or $J_{12} < 0$, resulting in the asymptotic forms of the resonance magnetic fields:

$$B_{21}/B_{31} = \frac{(g_1+g_2)h\nu}{2\beta g_1 g_2} - \frac{2(h_1+h_2)}{\beta(g_1+g_2)} - \frac{3}{8}A \pm \frac{2}{|J_{12}|}\left\{\left(\frac{h_1}{g_2} - \frac{h_2}{g_2}\right)^2 + \frac{A^2}{64}\right\} \qquad (33a/b)$$

and

$$B_{42}/B_{43} = \frac{(g_1+g_2)h\nu}{2\beta g_1 g_2} - \frac{2(h_1+h_2)}{\beta(g_1+g_2)} + \frac{3}{8}A - \frac{\pm2}{|J_{12}|}\left\{\left(\frac{h_1}{g_1} - \frac{h_2}{g_2}\right)^2 + \frac{A^2}{64}\right\}. \qquad (33c/d)$$

Notably, the fact that the effective hyperfine coupling fields of the second terms in eqs 33a-d are an arithmetic average of h_1/β and h_2/β represents a phenomenon of exchange narrowing [35]. Evidently, this limiting behavior coincides with the observed wings spreading over about a half range of the multiline signal. Then, the intensity of the EPR signal may depend on temperature T in proportion to the Boltzmann distribution function,

$[1+\exp(J_{12}/2k_BT)]^{-1}$, which tends to 1 when $-J_{12} >> k_BT$, and 0 when $J_{12} >> k_BT$. But, we remark that even at helium temperature k_BT may be still much larger than the J_{12} in this limit, resulting in a temperature-independent EPR signal.

4. The Effective Spin-Spin Interactions: J_{12} and D_{12}.

Both the exchange (J_{12}) and the magnetic dipolar ($\mathbf{D}_{12}$) interactions between the S_1=1/2 Mn-tetramer and its ligand radical can dramatically change depending upon the structural and electronic states of the Mn cluster. The flexibility of these spin-spin interactions mainly arises from the exchange interactions between Mn and radical spins, which are defined by (see Appendix B)

$$J_{i2} = -\frac{2}{2S_1+1}\sum_{k=1}^{2S_i}\int d\mathbf{r}_k \int d\mathbf{r}_2 d_k^* \psi_2(\mathbf{r}_k) \left\{\frac{e^2}{|\mathbf{r}_k - \mathbf{r}_2|} + K(\mathbf{r}_k,\mathbf{r}_2)\right\}\psi_2^* d_k(\mathbf{r}_2) \tag{34}$$

{i=a-d}, in which the second term represents all the possible superexchanges or "kinetic exchanges" [35], as well as the weak or intermediate superexchange interactions within the Mn-tetramer $\{J_{ij}, ij \neq ab\}$.

Firstly, we consider the "direct" or "potential" exchange term in eq 34: When orthogonal orbitals are assumed between an unpaired electron of the radical (Ψ_2) and the 3d-electrons of the ith Mn ion (d_k; k=1, 2,...,$2S_i$), each integral in eq 34, which is necessarily negative (ferro) because it is the self-energy of the (complex) charge distribution $d_k^*\Psi_2(\mathbf{r})$ ($\equiv d_k^*(\mathbf{r})\Psi_2(\mathbf{r})$) [35], can be reasonably estimated to be $\varepsilon_{k2}^2UC_{k2} \approx 1\times10^4\varepsilon_{k2}^2$ cm^{-1}, where ε_{k2} is a coefficient in the expansion $d_k=d_k^{(0)} - \varepsilon_{k2}\Psi_2 + \cdots$, U the interatomic Coulomb repulsion (≈ 13 eV) and C_{k2} a reduction factor due to the Mac-Weeny's theorem for the exchange integral (≈ 10^{-1})[35], so that we obtain

$$J_{i2} \approx -2\cdot10^4\cdot\frac{1}{2S_i+1}\sum_{k=1}^{2S_i}\varepsilon_{k2}^2(\mathrm{cm}^{-1}) + \text{superexchange terms;} \tag{35}$$

since a predominant ε_{k2} is likely of order 0.1 to 0.2, the first term is expected to be of order - 40 to -160 cm^{-1} for Mn(III) and -50 to -200 cm^{-1} for Mn(IV) ion. This estimation only gives the upper limit of ferromagnetic exchange interaction. In reality, however, some antiferromagnetic superexchange bipaths must be available, so that the effective J_{i2} may be substantially reduced and even overshoot to weak-antiferromagnetism (e. g. -20 cm^{-1} < J_{i2} < 20 cm^{-1}). Thus, we find that the J_{i2} must be quite sensitive to a modification of Ψ_2 due to the change of surrounding electrostatic field as well as a conformational change of ligand coordination.

Based on these findigs, we propose that the normal S_3-state would be EPR-silent because of its being in the singlet ground state with $J_{12} \gg k_BT$, while the modified S_3'-state would be inhomogeneous, involving at least three forms of the Mn clusters: form **1** and form **2** specified by $|J_{12}| \approx$ 100-200 G and 100-200 G « $|J_{12}|$ « k_BT, respectively, which would be minor components responsible for the doublet and wings in the S_3' signal, respectively, and from **3** with $J_{12} \gg k_BT$, which would be a major EPR-silent component, as was evidenced by the recent pulsed EPR experiment [22].

On the other hand, the magnetic dipolar interaction $\mathbf{D}_{i2}$ can take a magnitude ranging from 3210 G at r_{i2} = 2Å to 118 G at r_{i2} = 6Å. Since the doublet component indicates that the anisotropic interaction D_{12} must be as small as or less than the isotropic interaction $|J_{12}| \approx$ 100-200 G, the Mn cluster **1** must be in a "conformational substate (CS)" with a set of superexchange interactions $\{J_{ij}\}$ yielding a pair of vanishingly small effective Mn spins, either $\{P_aS_1, P_bS_1\}$ at $\theta_0 \approx \pm 60°$ or $\{P_cS_1, P_dS_1\}$ at $\theta_0 \approx 0°$ (see Fig. 1), to which the radical is directly bound at a site giving rise to no large residual anisotropy compared with the J_{12}. In the case of distorted trapezoid Mn-tetramers (which may be in general non-planar), which covers a large body of the Mn tetramers other than compact cubanes, there would be only two possible sites as depicted in Fig. 2 A and B, because the other binding sites must be accompanied by too large $\mathbf{D}_{12}$ of order 300-700 G mainly because of their shorter distances to the nearest Mn ion in another Mn pair: In model A, the radical constitutes the third bridge ligand between di(μ-oxo) bridged Mn(III) and Mn(IV) ions, and, in model B, it does some bridge ligand between the other Mn ions.

Model A :

i) The effective exchange interaction J_{12}

This is defined by eq 10 with eqs 13a-d and can be expanded around $\theta_0=\pm 60°$ as a linear function of θ_0:

$$J_{12} \approx J_0^A\sqrt{[(1-\eta)^2+\xi]}(\theta_0-\theta_J^A) \equiv J^A\Delta\theta_0, \qquad (36)$$

with

$$J^A \approx J_0^A = -\frac{2}{\sqrt{3}}(2J_{a2}-J_{b2})+\frac{1}{\sqrt{3}}(J_{c2}+J_{d2}) \pm 3p_{10}(J_{c2}-J_{d2}). \qquad (37)$$

$$\xi \equiv \frac{J_{c2}+J_{d2}}{\sqrt{3}J_0^A}, \qquad (38)$$

$$\eta \equiv \pm\frac{p_{10}(J_{c2}-J_{d2})}{J_0^A}, \qquad (38)$$

and

$$\theta_J^A = \pm\frac{\pi}{3}+\frac{\sqrt{3}}{2}\{1-\eta-\sqrt{(1-\eta)^2+\xi}\}, \approx \pm\frac{\pi}{3}+\frac{J_{c2}+J_{d2}}{8(2J_{a2}-J_{b2})} \qquad (39)$$

Thus, we find that J_{12} vanishes at $\theta_0=\theta_J^A$, which will be called " a magic phase angle ". θ_J^A must be close to $\pm$ 60° because, usually, $J_{c2} \ll |2J_{a2}-J_{b2}|$ and $J_{d2} \ll |2J_{a2}-J_{b2}|$, but its deviation from ±60° would be by no means negligible because, for instance, it amounts to 2.7° even for ξ =-0.1 and η =0.0. The present theory has the great advantage of the flexibility of parameter $|2J_{a2}-J_{b2}|$, which can take the value of order ranging from 1 cm^{-1} to 100 cm^{-1}, depending on how the molecular orbital of the radical spin is extended along the bridge. The other flexible parameter is $\Delta\theta_0 = \theta_0 - \theta_0^A$, which is a sensitve function of all the exchange interactions, $\{J_{ij}\}$ and $\{J_{i2}\}$, and can take any value if the Mn cluster is appropriately modified. For instance, we can reasonably imagine that the values of J_0^A and $\Delta\theta_0$ are of order, ±1 cm^{-1} and ±0.5°, ±10 cm^{-1} and ±10°, and 100 cm^{-1} and ±10° in the Mn_4-radical complex in form **1**, **2**, and **3**, respectively. In Fig. 3, we plot the J_{12} vs $\Delta\theta_0$ relations for some reasonable values of J^A. A remarkable reduction of the effective interaction should be noted: e.g. J_{12} = 0.015 cm^{-1} (experimental) is obtained from J^A=1 cm^{-1} by assuming $\Delta\theta_0$=0.9°, which is likely enough to happen.

Next, we ask what conformational change has occurred in the Mn-radical complex **1**. In Ca^{2+}-depleted PSII membranes, a change of the phase angle θ_0 from ca. -45° (this choice of branch corresponds to the case of J_- > 0 in the ground state) to ca. -60° upon the $S_2' \rightarrow S_3'$ transition is found from eq 6 to be equivalent to a change

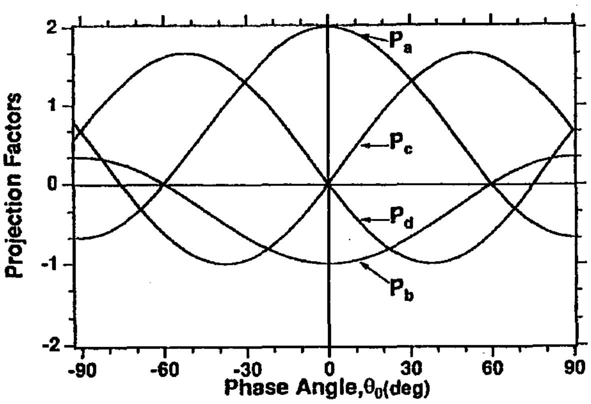

Fig.1 EPR hyperfine projection factors vs the phase angle θ_0 representing a spin-hybridization between S_{cd}=0 and S_{cd}=1 composite spin eigenvectors, in a Mn_4(III,IV,IV,IV) complex with the other composite spin S_{ab}=1/2 fixed to give a total spin S_1=1/2.

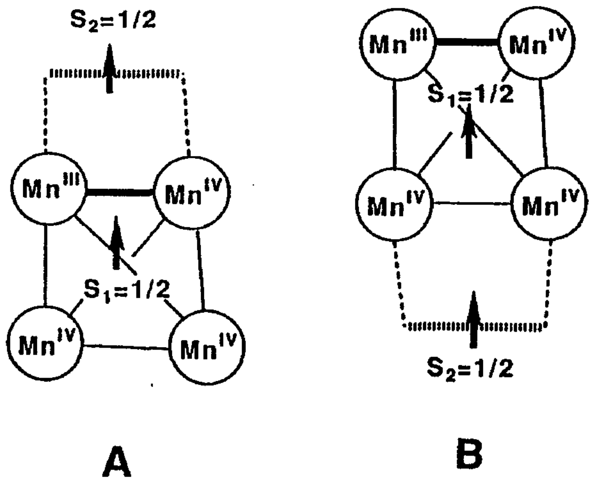

Fig.2 Two possible ligation models A and B of an unknown radical whose spin S_2=1/2 can very weakly interact with a spin S_1=1/2 of the Mn_4(III,IV,IV,IV) tetramer, defined in Fig.1 legend, at $\theta_0 \approx \pm$ 60° (A) or $\approx$ 0°(B).

from

$$J_{cd} \approx J_+ = (J_{ad} - 0.5J_{bd}) + (J_{ac} - 0.5J_{bc}) \text{ ; in the } S_2'\text{-state}$$

to

$$J_{cd}' \approx J_+' + \sqrt{5}J_-' = \{1-\sqrt{5}\}(J_{ac}' - 0.5J_{bc}') + \{\sqrt{5}+1\}(J_{ad}' - 0.5J_{bd}') \text{ ; in the } S_3'\text{-state,}$$

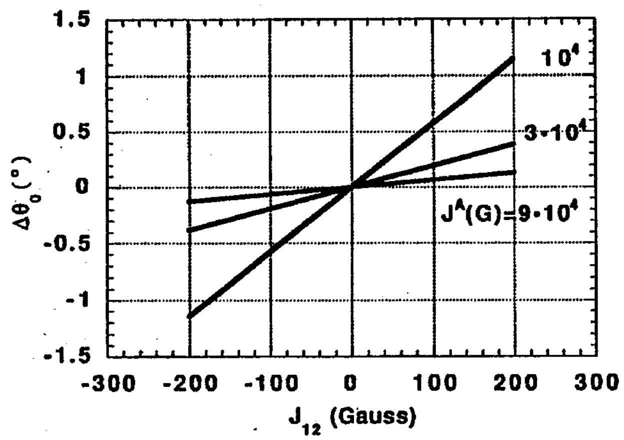

Fig.3 The effective exchange interaction J_{12} as a function of $\Delta\theta_0 = \theta_0 - \theta_J^A$, showing a remarkable reduction from the native one (J^A) which can take a value of order 1 cm^{-1} when $2J_{a2}$ and J_{b2} largely cancel out.

with the ground-state condition: $J_{ac} + 0.5J_{bd} > J_{ad} + 0.5J_{bc}$ and $J_{ac}' + 0.5J_{bd}' > J_{ad}' + 0.5J_{bc}'$. If the Mn tetramer takes a form of the distorted trapezoid ($J_{ad} \approx J_{ad}' \approx 0$ and $J_{bc} \approx J_{bc}' \approx 0$), these relations reduce to $J_{cd} \approx J_{ac} - 0.5 J_{bd}$ in S_2' and $J_{cd}' \approx -1.24J_{ac}' - 1.62 J_{bd}'$ in S_3', indicating that a significant conformational change must occur upon the $S_2' \rightarrow S_3'$ transition. If the Mn cluster takes another possible form of trimer plus monomer with $J_{ad} \approx J_{bd} \approx 0$, these relations reduce to $J_{cd} \approx J_{ac} - 0.5J_{bc} > 0$ in S_2' and $J_{cd}' \approx -1.24(J_{ac}' - 0.5J_{bc}') < 0$ in S_3', indicating that J_{cd} must change from antiferromagnatic to ferromagnetic upon this transition.

ii) The magnetic dipolar interaction: D_{12}

Boussac et al.[23] observed that the doublet lineshape of the S_3' signal is significantly close to symmetric, and were obliged to assume that the dipole-

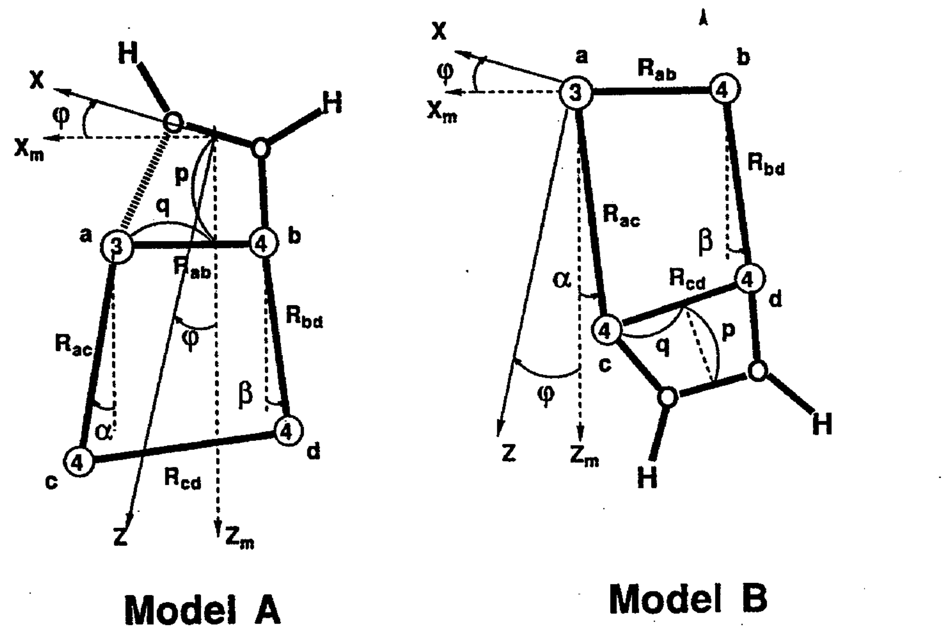

Fig.4 Definition of eight structural parameters in two possible models A and B of the Mn_4(III,IV,IV,IV)-radical complex which is assumed to be planar, for simplicity. Each model is subdevided into several plausible submodels defined in Table 1.

dipole interaction would result in only a broadening rather than a splitting of the radical signal. The fact that the splitting is a result of a correlated motion of the two half spins indicates that the assumption mentioned above would be valid only when the dipole-dipole interaction D_{12} is smaller than the isotropic exchange interaction J_{12}. Therefore, the $\mathbf{D}_{12}$ tensor should play another key role on the structure study of the Mn_4-radical complex **1** in the S_3'-state.

In order to demonstrate how the ZFS parameters D_{12} and E_{12} approach zero around $\theta_0 \approx -60°$, we would adopt a planar trapezoid structure for the Mn_4(III,IV,IV,IV) tetramer as illustrated in Fig. 4, where a radical, $(HOOH\cdot)^-$, is assumed to be the most probable bridging ligand, which will be justified later, and the principal XYZ axes are related to the molecular X_mYZ_m axes by a rotation φ around the common Y-axis, with the X_m-axis taken along the $Mn_b(IV) \rightarrow Mn_a(III)$ direction. Also, we define eight structural parameters: $\{R_{ij}$; ij=ab, ac, bd, cd$\}$, p, q, α_1 and α_2. Here, we would consider only two possible submodels; **A1** being symmetric and compact, and **A2** being asymmetric and loose (a dimer-of-dimers model cannot belong to model **A**, but to model **B**), and, in each submodel, we would have three possible radical binding sites whose structural parameters are defined in Table 1. For these six submodels of model **A**, the calculated D_{12} vs θ_0 (thick solid line), E_{12} vs θ_0 (thick dotted line) and φ vs θ_0 (thin solid line) relations are plotted in Fig. 5, a through f. It should be noted that φ has been limited in the range, 0

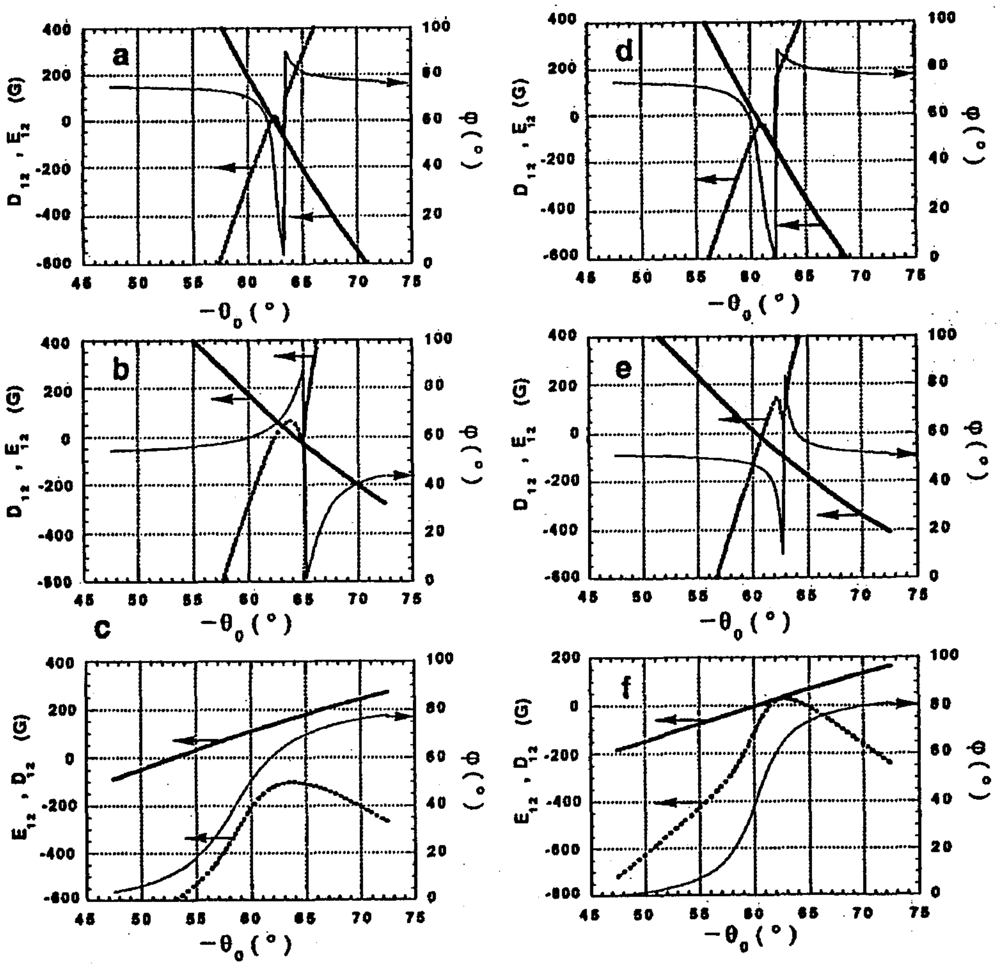

Fig.5 The magnetic dipolar interaction $\mathbf{D}_{12}$ as a tensor function of θ_0 involving the D_{12} vs θ_0(thick solid line), E_{12} vs θ_0 (dashed line) and φ vs θ_0 (thin solid line) relations in possible submodels of model A: (a) **A1a**, (b) **A1b**, (c) **A1c**, (d) **A2a**, (e) **A2b** and (f) **A2c** (see Table 1).

$\leq \varphi \leq \pi/2$, so that E_{12} may change the sign when φ crosses over either boundary of φ=0 or $\varphi=\pi/2$. It follows; (1) The D_{12} vs θ_0 relation is an almost straight line which intersects the D_{12}=0 axis at $\theta_0 = \theta_D$ near -60° and yields the $|D_{12}|$ value less than 50 G in the the range, $|\theta_0 - \theta_D| < \Delta\theta_D$, depending upon the cluster conformation and the center of radical spin. The values of θ_D and $\Delta\theta_D$ are tabulated in Table 1. The narrower the range of this small $|D_{12}|$ is, the lower the probability of such a Mn-radical complex is. Furthermore, the magic phase angle $\theta_J{}^A$, which is expected to be at most ± 6° apart from -60°, must lie in this range of θ_0. Therefore, from the standpoints of D_{12} and $\theta_J{}^A$, we conclude that the most probable Mn_4-radical complex would be submodel **A2c**, which binds the radical at the Mn_b(IV) site, as depicted in Fig.4A. (2) The rhombic component E_{12} takes a local maximum at slightly above -60° and, if the local maximum value is larger than -50 G, there must appear some ranges of θ_0 defined by $|\theta_0 - \theta_E| < \Delta\theta_E$ in which E_{12} takes the magnitude less than 50 G, as given in Table 1. As far as this E_{12} is concerned, submodel **A2c** would be most likely because it shows much larger $\Delta\theta_E$ (=2.9°) than the other models (0.25°-0.6°). (3) *Significantly, these regions of θ_0 giving rise to the small* anisotropic interactions show a rather large overlap in the range, $60.7° < -\theta_0 < 64.0°$, which significantly coincides with the possible range of $\theta_J{}^A$ estimated from eq 40 with usual conditions $0 < J_{c2} + J_{d2} \ll 2J_{a2} - J_{b2}$. Also, it should be noted that only this radical binding site can be consistent with a small $|J^A|$. Therefore, we conclude that the Mn tetramer may consist of a di (μ-oxo) Mn_2 (III,IV) dimeric subunit and the other two monomeric Mn(IV) ions that are somewhat loosely and asymmetrically organized, and also, the radical would be more strongly bound to Mn_b(IV) site than to Mn_a (III) site in the Mn_2 (III,IV) dimer.

Model B :

i) The effective exchange interaction J_{12}

In model **B** with $\theta_0 \approx 0$ (Fig.2), J_{12} given by eq 10 with eqs 12a-d can be expanded as a power series of θ_0 and approximated as

$$J_{12} \approx J^B(\theta_0 - \theta_J^B) \equiv J^B \Delta\theta_0, \tag{41}$$

with

$$J^B = 2p_{10}(J_{c2} - J_{d2})\sqrt{1-\zeta},$$
$$\zeta = \frac{(2J_{a2} - J_{b2})(J_{c2} + J_{d2} - 4J_{a2} + 2J_{b2})}{3p_{10}{}^2(J_{c2} - J_{d2})^2} \tag{42}$$

and

$$\theta_J^B = \frac{3J^B\{1 - [1-\zeta]^{-1/2}\}}{4(J_{c2} + J_{d2} - 4J_{a2} + 2J_{b2})} \approx -\frac{(2J_{a2} - J_{b2})}{4p_{10}(J_{c2} - J_{d2})}. \tag{43}$$

Table 1 Possible Mn-radical complexes in the S3 and S3' states, each taking a structural conformation with a small magnetic dipolar interaction between the radical (HOOH•)- and Mn-tetramer spins in the cited θ0 regions for the axial (D12) and rhombic (E12) components to become less than 50 G in magnitude (see Figs 5 and 6).

Structure Parameters	Models								
	A1			A2			B		
	a	b	c	a	b	c	a	b	c
[Rab, Rcd, Rac, Rbd](Å) [α1, α2](°)	[2.7, 3.62, 3.3, 3.3] [8, 8]			[2.7, 4.1 , 5.0, 3.3] [10, 4]			[2.7, 2.73, 4.2, 3.3] [-8, 8]		
p(Å) q(Å)	0.6 2.1	1.35 1.86	2.1 2.1	0.6 2.1	1.35 1.86	2.0 2.0	0.6 2.1	1.35 1.86	2.1 2.1
− θD ± ΔθD(°)	62.3 ±0.7	64.3 ±1.3	53.1 ±3.2	60.5 ±0.6	60.4 ±1.3	55.4 ±8.6	-2.2 ±1.1	0.90 ±0.5	0.25 ±0.1
− θE ± ΔθE(°)	62.4 ±0.6	62.6 ±0.6 64.6 ±0.3	—	61.0 ±0.3	61.0 ±0.5	63.6 ±2.9	-0.75 ±0.25	—	—

Thus, the J_{12} vs θ_0 relation is found to intersect the θ_0-axis at $\theta_0 = \theta_J{}^B$, "a magic phase angle", which may be usually slightly below θ_0=0 in either radical binding site of Mn_c(IV) or M_d(IV) ion, accompanied by the relations, $0 < J_{b2} < 2J_{a2} << J_{d2} < J_{c2}$ and $0< 2J_{a2} < J_{b2} \ll J_{c2} < J_{d2}$, respectively.The value of J^B would be of the same order of magnitude as J^A , so that Fig. 3 may be used with replacement of parameter J^A of J^B to determine J_{12} from $\Delta\theta_0$.

In contrast to model A, however, model B is required to satisfy a more severe condition for the intra-tetramer exchange interactions, as given from eq 6 by

$$\left|\frac{3p_{10}J_-}{2(J_{cd}-J_+)}\right| \approx |\theta_0| \langle\langle \frac{\pi}{2}: \qquad (44)$$

which is mostly equivalent to $J/J_{cd} \approx O\ (10^{-2})$, implying that the $S_2' \rightarrow S_3'$ transition should result in either case of $J_- \approx J_{ac} + J_{bd}/2 \approx O$ (0.1-0.01 cm^{-1}) or $J_{cd} \approx O$ (10^2 cm^{-1}). The former is much less probable than the latter, because the former requires an additional condition, i.e. a sign change of J_{ac} or J_{bd} from antiferromagnetic to ferromagnetic, although even the latter can hardly take place. Furthermore, the bridging radical must add a ferromagnetic contribution to J_{cd}, making the latter less probable. Nevertheless, it would be interesting to know whether a dimer-of-dimers model, which satisfies eq 44, is consistent or not with the observed small anisotropic interaction in the S_3' signal.

ii) The magnetic dipolar interaction $\boldsymbol{D}_{12}$

In Table 1, we have presented structural parameters for a typical dimer-of-dimers model combined with the three possible radical binding sites, called "submodels **Ba**, **Bb** and **Bc**", and the resultant ranges of θ_0 which give rise to small axial and rhombic dipolar interactions, i.e. $|D_{12}| < 50$ G in the range $|\theta_0\text{-}\theta_D| < \Delta\theta_D$ and $|E_{12}| < 50$ G in the range $|\theta_0\text{-}\theta_E| < \Delta\theta_E$, respectively. The bare D_{12} vs θ_0, E_{12} vs θ_0 and φ vs θ_0 relations are depicted in Fig. 6 a, b and c, to show that only submodel **Ba** can take a small rhombic dipolar interaction, $|E_{12}| < 50$ G, in a narrow range, -1.0° < θ_0 < -0.5°, but this range does not overlap with that (- 3.35° < θ_0 < -1.05°) for small axial dipolar interaction, $|D_{12}|$ < 50 G. Thus, we conclude that the dimer-of-dimers model must exhibit some appreciable anisotropic features in the S_3' signal.

5. Numerical analysis of the S_3' signal

The observed S_3' signals seem to consist of two distinguishable components: a narrow doublet with 100-200 G wide splitting and a broad wings extending over 2950-3860 G at X-band frequencies [19]. The doublet spectrum was computer-simulated by Boussac et

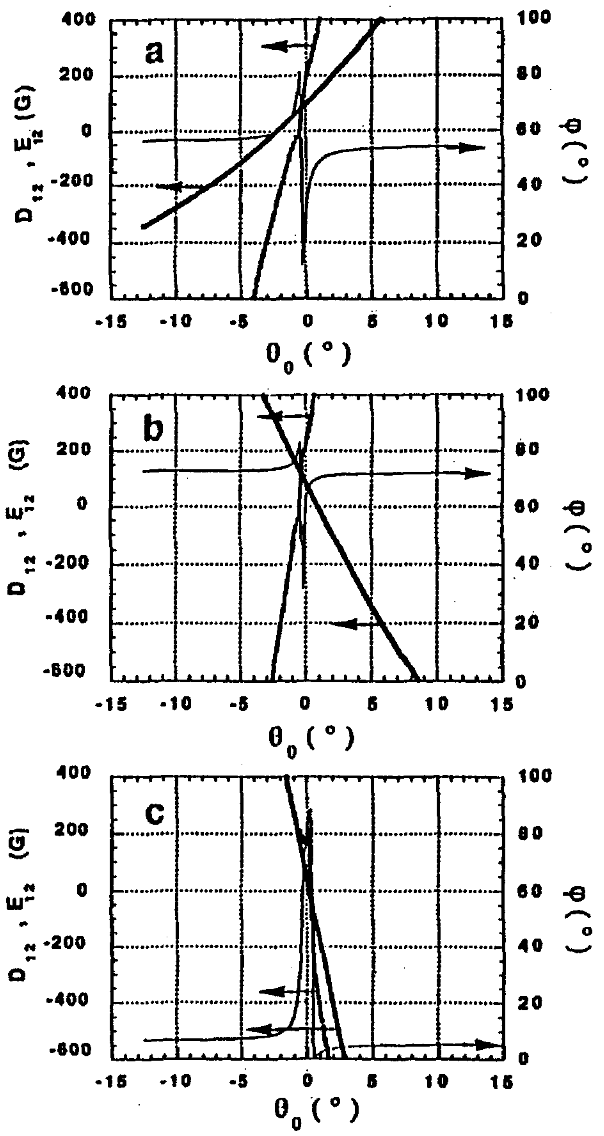

Fig.6 The same relations as in Fig. 5 in possible submodels of model B: (a) **Ba**, (b) **Bb** and (c) **Bc** (see Table 1).

al.[23]: the stick spectrum obtained from a set of parameters (A_a=150 G, A_b=75 G, A_c=52.7 G, A_d=48.6 G, g_1=1.965, g_2=2.012, J_{12}=67.4 G and $\mathbf{D}_{12}$=0) had to be convoluted with different Gaussian line shape functions with large broadening, ΔB_1=40 G and ΔB_2=43 G, for the Mn-tetramer and radical lines, respectively. It was found that the multiline component due to the Mn-tetramer becomes unresolvable and collapses to a level much weaker than the observed wings. This discrepancy originates from the His-radical hypothesis that limits the value of J_{12} to such a weak level. Furthermore, Boussac et al.[23] assumed that $\mathbf{D}_{12}$ might have contributed not to the energy level splitting but to the line broadening capable to be incorporated into the Gaussian broadening function. However, this assumption should be allowed only for powdered spectra in an inconsistent case where both D_{12} and E_{12} of long-range nature are much smaller than J_{12} of short-range nature.

This section is devoted to numerically demonstrating how reasonably the present hypothesis

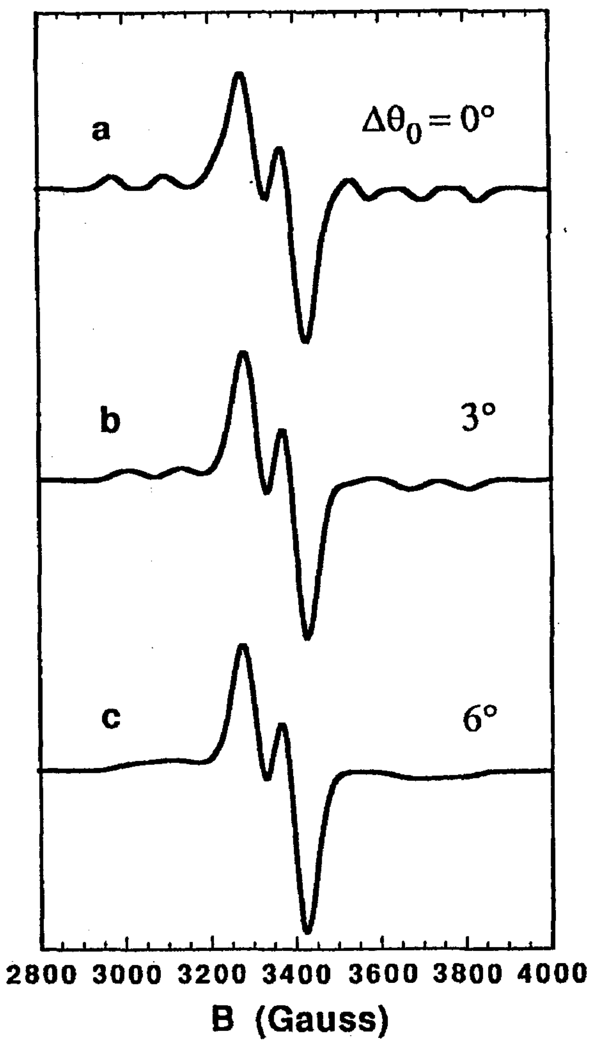

Fig.7 The effect of the magic phase angle θ_J^A on the EPR signal from the Mn_4- radical complex **1** with J_{12} =0.015 cm^{-1} and $\mathbf{D}_{12}$=0 (the spectroscopic parameters are ν=9.4 GHz, g_1=1.98, g_2=2.011, a_a= -96 G, a_b=-77 G, a_c=-.83 G, a_d=-81 G and ΔB^*=25 G): $\Delta\theta_J^A=\theta_J^A + 60° = 0°$ (a), 3° (b) and 6° (c).

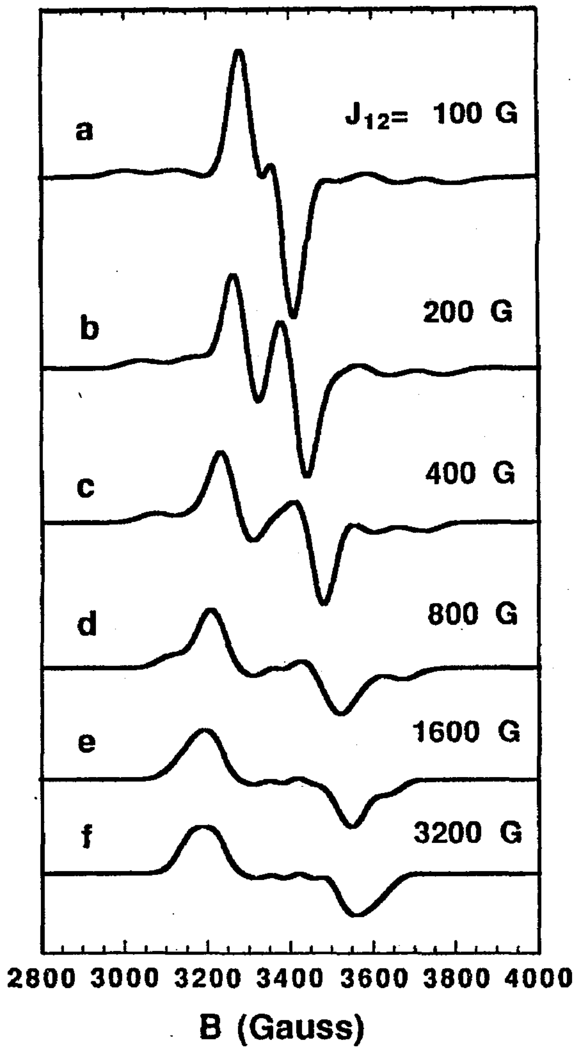

Fig.8 The effect of the effective exchange interaction J_{12} on the EPR signal from the Mn_4-radical complex with the same spectroscopic parameters as in Fig.7, except θ_0=-65°.

can explain all the features in the S_3' signal.

(i) The effect of the magic phase angle $\theta_J{}^A$ on the multiline component

The wings of the S_3' signal do not exhibit any resolved multilines due to Mn-nuclear hyperfine splittings. This fact can be regarded as an evidence of the tetra-nuclear Mn complex, because, if the Mn complex is a dimer, the S_3'signal must show an observable hyperfine structure similar to that depicted in Fig.7 a. Therefore, the essential factor behind this fact would be a deviation of the magic phase angle $\theta_J{}^A$ from -60° in model A. In the previous sections, it was shown that this deviation arises from the non-vanishing exchange interactions between the radical and distant Mn spins, that is, J_{c2} and J_{d2}, and can possibly reach 3-6°. In Fig. 7, we plotted the theoretical S_3' signals as a function of $\Delta\theta_J{}^A = \theta_J{}^A + 60°$ (=0°, 3° and 6°) to be observed from a probable Mn-radical complex **1** with fixed J_{12}=0.015 cm^{-1} and $\mathbf{D}_{12}$=0, where the following spectroscopic parameters were adopted: ν=9.4 GHz, g_1=1.98, g_2=2.012, a_a= -96 G, a_b= -77 G, a_c= -83 G, a_d= -81 G and ΔB^*=25 G. A remarkable finding is that the multiline fearture, which is clearly resolved at $\Delta\theta_J{}^A$=0°(Fig.7a), rapidly disappears as $\Delta\theta_J{}^A$ only slightly increases (Fig.7b and c). This can be reasonably explained as the line broadening effect due to the recovering hyperfine couplings at Mn_a(III) and Mn_b(IV) nuclei. We would emphasize that four independent estimates of the allowed θ_0 regions from the $\theta_J{}^A$ itself (eq 40), $|D_{12}|$ < 50 G, $|E_{12}|$ < 50 G (Table 1) and the line broadening effect (Fig. 7) contain an overlapping region between -62° and -64°, only in submodel **A2c**. Moreover, we find that the collapsed multiline feature in Fig. 7c is too weak to explain the observed appreciable intensity of the wing component.

(ii) The effect of the effective exchange interaction J_{12}

In order to remove this discrepancy, we must assume that, in the S_3' state, the Mn clusters are inhomogeneously disturbed to generate a distribution of J_{12} in a wide range of magnitude. In Figs 8 a through f, we show the theoretical EPR spectra as a function of $|J_{12}|$, where we used for simplicity the same set of parameters as in Fig. 6 except θ_0 being fixed at -64°. It is found that, when the J_{12} is small, the S_3' signal becomes a sharp doublet with the peak-to-peak width of ~ $|J_{12}|$ (see Fig. 8a for $|J_{12}|$=100 G and 8b for $|J_{12}|$=200 G); as $|J_{12}|$ increases, the doublet splitting becomes wider and weaker while the collapsed multiline component starts to grow (see Fig. 8c for $|J_{12}|$=400 G and 8d for $|J_{12}|$=800 G); when $|J_{12}|$ exceeds the spectral width, these doublet and multiline components consolidate and form a very broad and weak doublet spectrum similar to the wings of the S_3' signal (see Fig. 8e for $|J_{12}|$=1600 G and 8f for $|J_{12}|$=3200 G). This limiting behavior represents the effect of exchange narrowing and has been discussed in Section 3 (see eqs 33a-d). In this limit, the width of the signal is approximately given by a half of that of the dark stable multiline signal in the S_2' state, in agreement with an observation (≈ 910 G[19] ≈ 1700 G[23] /2) Thus, we conclude that the wings of the S_3'signal should have arisen from the Mn-radical complexes with strong effective exchange interaction satisfying 200 G << J_{12}< k_BT, where the second inequality is required from the Boltsmann distribution function as will be discussed below.

Therefore , a correct computer simulation of the observed S_3' signal requires a knowledge on the distribution function of J_{12} as given by

$$\rho(J_{12}) = \sum_k \frac{w_k}{\sqrt{2\pi\Delta J_k}} \exp\left[-\frac{(J_{12}-J_k)^2}{2\Delta J_k^2}\right], \tag{45}$$

where w_k represents a fractional population of the enzyme-substrate complexes in the k-th conformational substates corresponding to a group of local-minimum-energy conformations, and these Mn-radical complexes are supposed to be in a Gaussian distribution of J_{12}, centered at J_{12}=J_k with width ΔJ_k. Let $A_{ij}(B,\Delta B,J_{12})$ be the EPR absorption spectrum due to the i → j transition (ij=31, 42, 21, 43) with ΔB being the inhomogeneous broadening at J_{12}=0. Then, the total mean absorption spectrum is approximately given by

$$\overline{A(B)} = \int_{-\infty}^{\infty} dJ_{12}\,\rho(J_{12}) \sum_{(ij)} A_{ij}(B,\Delta B,J_{12})\left[1+\exp\left(\frac{J_{12}}{2k_BT}\right)\right]^{-1},$$

$$\approx \sum_k w_k\left[1+\exp\left(\frac{J_k}{2k_BT}\right)\right]^{-1} \sum_{(ij)} A_{ij}(B,\Delta B_{ij}^k,J_k) \tag{46}$$

where we introduced a total inhomogeneous broadening ΔB_{ij}^{k} associated with the i $\rightarrow$ j transition of the k-th group of the Mn-radical complexes. These ΔB_{ij}^{k} can be estimated from eqs 46 and 29a-d with eqs 30a-b and 31a-c as follows: (1) $\Delta B_{ij}^{d} \approx \Delta B_d = \sqrt{(\Delta B^2 + \Delta J_d^2/4)}$ for the doublet components, (2) $\Delta B_{31}^{w} = \Delta B_{43}^{w} \approx \Delta B_w = \sqrt{(\Delta B^2 + \Delta J_w^2)}$, $\Delta B_{42}^{w} = \Delta B_{21}^{w} \approx \Delta B$ *for the wing* components with $J_w \gg \sqrt{(\langle h_1^2\rangle)}$, and (3) $\Delta B_{31}^{w} = \Delta B_{43}^{w} \approx \Delta B$, $\Delta B_{42}^{w} = \Delta B_{21}^{w} \approx \Delta B_w = \sqrt{(\Delta B^2 + \Delta J_w^2)}$ for the wing components with $J_w \ll -\sqrt{(\langle h_1^2\rangle)}$.

This picture provides a quite reasonable interpretation of recent pulsed EPR measurements [22] showing that the S_3' signal presents only 23 % of the integrated EPR signal area of the S_3 - state multiline signal: the remaining EPR-silent centers must be in singlet states with $J_{12} \gg k_BT$. In addition, the S_3' signal reported by Andréason et al.[19] exhibits a pair of shoulder peaks on the doublet spectrum, indicative of coexistence of the Mn_4-radical complexes with $|J_k| \approx 153$ G and ≈ 278 G. Thus, we arrive an conclusion that the Mn-radical complexes must be inhomogeneous with respect to the effective exchange interactions, involving at least three groups: (1) $|J_{12}|$=100-300 G, (2) 100-300 G $\ll |J_{12}| < k_BT$, and (3) $J_{12} \gg k_BT$.

(iii) The effect of the magnetic dipolar interaction D_{12}

As shown above, both D_{12} and E_{12} can be nearly quenched when the Mn-radical complex is essentially described by the model **A2c** as depicted in Fig. 4A, although the quenching would be in general incomplete. The residual anisotropic interactions may be detected by careful and accurate measurements on the orientation dependence of the doublet component with use of the oriented PSII membranes. In Fig. 9, we define and illustrate the relevant coordinate axes and angles needed to describe the membrane EPR phenomenon: The applied magnetic field **B** makes a polar angle θ_B relative to the membrane normal (z'-axis) and lies in the x'y'-plane of the laboratory frame; the principal z-axis of tensor $\mathbf{D}_{12}$ makes polar angles θ_D, ϕ with respect to the x'y'z'-coordinate system and the principal x-axis does a rotation angle ξ from the zz'-plane, resulting in the azimuthal angle φ of **B** in the principal xyz coordinate system as given by

$$\cos\varphi = [\sin\theta_B(\sin\xi\sin\phi - \cos\xi\cos\theta_D\cos\phi) + \cos\theta_B\sin\theta_D\cos\xi]/\sin\theta \quad , (47)$$

with the addition theorem of Legendre functions,

$$\begin{aligned}\cos^2\theta - \frac{1}{3} = \frac{3}{2}(\cos^2\theta_B - \frac{1}{3})(\cos^2\theta_D - \frac{1}{3}) \\ + \frac{1}{2}\sin 2\theta_D \sin 2\theta_B \cos\phi \\ + \frac{1}{2}\sin^2\theta_D \sin^2\theta_B \cos 2\phi\end{aligned} \quad , \quad (48)$$

which describes the angular dependence of the axial component of $A(\theta,\varphi)$ in eq 19. Similarly, the rhombic component of $A(\theta,\varphi)$ is proportional to

$$\begin{aligned}\sin^2\theta\cos 2\varphi = 3(\cos^2\theta_B - \frac{1}{3})(\cos^2\xi - \frac{1}{2})\sin^2\theta_D \\ + \sin 2\theta_B(\sin 2\xi \sin\theta_D \sin\phi - \frac{1}{2}\cos 2\xi \sin 2\theta_D \cos\phi) \\ - \sin^2\theta_B\{\cos\theta_D \sin 2\xi - \frac{1}{2}\cos 2\xi(1+\cos^2\theta_D)\}\cos 2\phi\end{aligned} \quad . \quad (49)$$

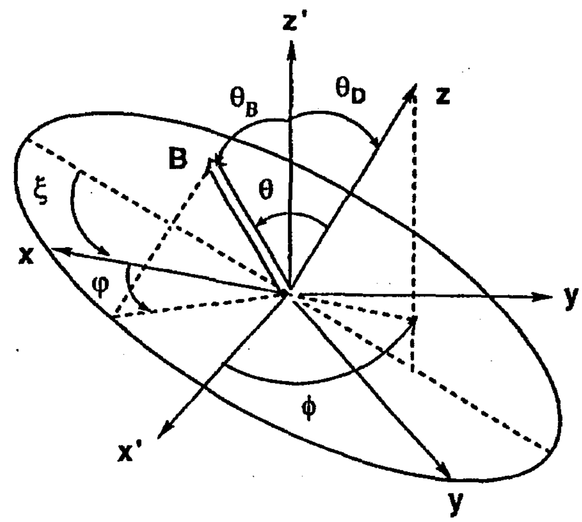

Fig.9 Defintion of a molecular coodinate system [xyz] *relative to the laboratory frame* [x'y'z']: the z'-axis represents the membrane normal, the direction of the applied magnetic field **B**, is defined by angles (θ_B, 0) and (θ, φ) in [x'y'z'] and [xyz], respectively, the direction of $\mathbf{D}_{12}$ in [x'y'z'] by angles (θ_D, ϕ), and angle ξ gives the rotation angle of the x-axis from the zz' plane.

Since the oriented PSII membranes have no order with respect to a rotation ϕ around the membrane normal, all the terms in eqs 47 and 48 proportional to $\cos\phi$, $\sin\phi$ and $\cos 2\phi$ can cause only a line broadening as far as D_{12} and E_{12} are small, and the other terms can do a θ_B-dependent level shift. As a distinctive feature to the two-half spins system, we find two "magic angles" for θ_D and ξ, i.e. 54.7° and 45°, respectively, at which the axial and rhombic components in the θ_B-dependent level shift vanish, and there remains only an inhomogeneous line broadening due to

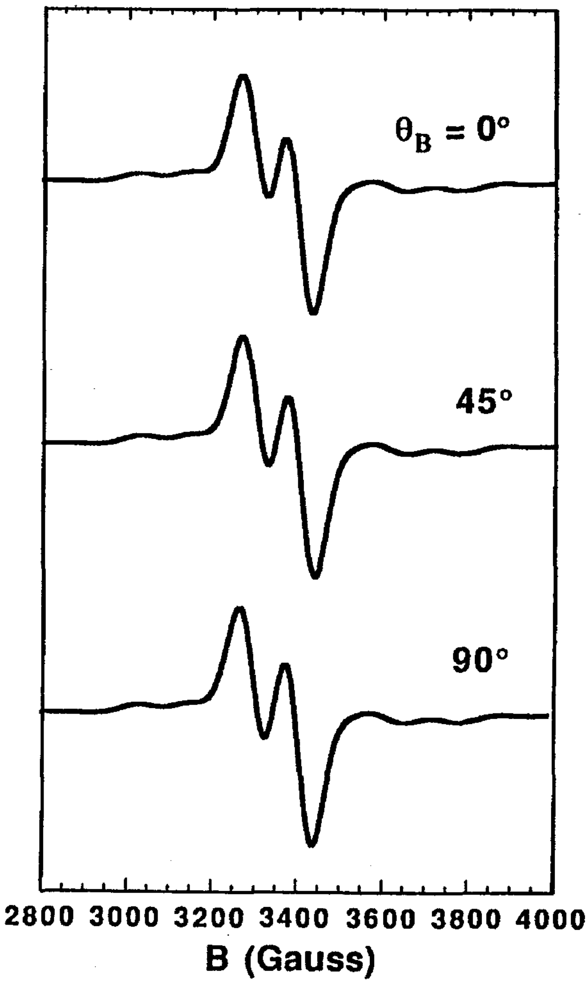

Fig.10 A predicted orientation dependence of the EPR signal from the model **A2c** Mn_4-radical complex in Ca^{2+}-depleted PS II membranes (see text) whose principal axes of $\mathbf{D}_{12}$ tensor are assumed to be oriented near $\theta_0 \approx -66°$ and $\xi = 20°$. The indicated angle is θ_B defined in Fig. 9.

$$A_m(\theta,\varphi) = \left(\frac{1}{\sqrt{3}}D_{12}\cos\phi + \sqrt{\frac{2}{3}}E_{12}\sin\phi\right)\sin 2\theta_B + \frac{1}{3}(D_{12} - \sqrt{3}E_{12})\sin^2\theta_B\cos 2\phi \tag{50}$$

It should be noted that this magic angle effect will become significant whenever $|\theta_D|$ and $|\xi|$ are not so far (possibly, within ± 15°) from 57.4° and 45°, respectively. This is partly because the membranes can not avoid a partial disorientation due to mosaic spread.

For instance, in the case of model **A2c** with J_{12}=150 G, D_{12}=38.8 G and E_{12}=26.5 G at $\theta_0 \approx -63°$, we may put $\theta_D \approx \varphi = 66.16°$ and $\xi \approx 20°$ as likely assumptions based on recent EXAFS data indicating that the 2.7 Å and 3.3 Å Mn-Mn bonds would be perpendicular and parallel to the membrane normal, respectively [4]. In Fig. 10, we show the orientation dependence of the S_3' signals at θ_B=0°, 45° and 90°, respectively, which arise from this Mn_4-radical complex specified by the same set of the other parameters as utilized in Fig. 7. Thus, we find that the orientation dependence of the peak position must be so weak if the present theory is correct.

(iv) EPR Spectral Simulations

The condition of small dipolar interaction for the doublet component was found to be most satisfied by such a model **A2c** Mn cluster with $-\theta_0 \approx$ 61-64° as depicted in Fig. 4A: in this model, the center of the radical spin surprisingly coincides with a middle point of the ≈1.46 Å O-O bond in the radical, $(HOOH\cdot)^-$, which is reasonably presumed to be more strongly bound on the Mn_b(IV) site than on the Mn_a(III) site to form an asymmetric third bridging ligand in the di-μ-oxo bridged Mn_a(III)-Mn_b(IV) dimeric subunit. The other possibility of an $HOHOH\cdot$ radical as the third bridging ligand is much lower, because a hydrogen bond in this ligand would be very short (< 2.50 Å) and near-symmetric [36] and hence the center of the radical spin must be described by the much-less-probable model **A2b**. Circumstantial evidences preferring model **A2c** may be provided by the following experimental findings: (1) a

UV absorption spectrum induced by flash illumination of dark-adapted Ca^{2+}-depleted PSII is similar [23] to that generated by the covalent addition of an OH· radical to His in aqueous solution at pH 9.2 [24], which may be in turn similar to the (HOOH·)$^-$ radical covalently bonded to the di(μ-oxo)Mn_2(III,IV) subunit (see Section 6); and (2) Mn K-edge XANES spectra induced by a series of flash illumination of the Ca^{2+}-depleted PSII membranes

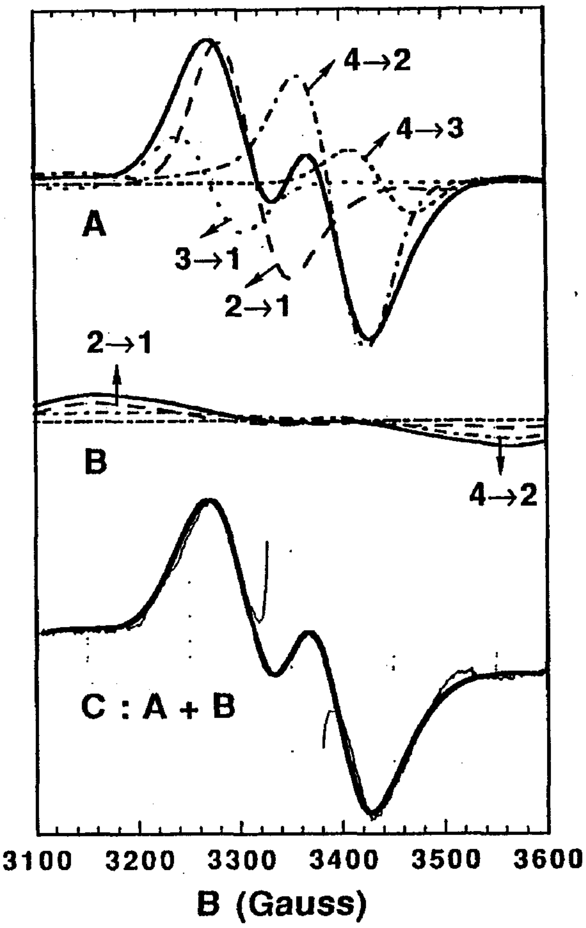

Fig.11 The best simulation of an observed S_3' signal 23(ν=9.4 GHz), based on the binary model of J_{12}-ditribution: i.e. {$J_d \approx 135$ G, $\Delta B_d \approx 29$ G, $w_d \approx 0.65$, $\theta_{od} \approx -65°$} and {$J_w \approx 2800$ G, $\Delta J_w \approx 201$ G, $w_w \approx 0.35$, $\theta_{ow} \approx -50°$} for the doublet and wing components, respectively. Both the doublet (A) and the wing (B) components (thick solid lines) are decomboluted into four transitions (non-solid lines). See text for the other parameters. (C) The theoretical (thick solid line) and experimental (thin solid line) spectra.

showed an abnormal stepwise upshift of the K-edge energy, i.e. ≈ 1.0 eV by one flash upon the S_1' to S_2' transition and ≈ 0.9 eV in total by many flashes to reach a steady state, possibly S_3' state [29], indicating that a Mn(III) or Mn(IV) ion, or its direct ligand in the Mn cluster could be oxidized up to two electrons but further events were blocked: the same conclusion was derived for the normal S_2 to S_3 transition too[28].

In spite of the possible multi-component origin of the wings of the S_3' signal, the EPR spectral simulations based on a binary model of J_{12}-distribution, which involves two sets of parameters, {J_d, ΔB_d, w_d, θ_{0d}} for the doublet component and {J_w, ΔB_w, w_w, θ_{0w}} for the wing component in eq 46, will provide useful information not only on J_d (≈100-200 G) and ΔB_d but also on the relative population w_d/w_w, provided that $\theta_{0d} \approx -65°$ (see above), and representatively; $\theta_{0w} \approx -50°$, $J_w \approx 2800$ G (» J_1), and $\Delta B_w \approx 200$ G (≈ $\Delta J_d{*}J_w/J_d$). In addition, the hyperfine coupling constants of four Mn ions {a_i ; i=a-d} are taken as equal to the previous ones, and those of two protons {a_k ; k=e,f} in the (HOOH·)$^-$ radical are for simplicity assumed to be equally a half of that in a hydroxyl radical [37]: i.e. $a_e \approx a_f \approx 20$ G. As depicted in Fig. 11, a powdered S_3' signal (a thin solid line in C) reported in ref 23 was best simulated to obtain an important set of parameters, {$g_1 \approx 1.98$, $g_2 \approx 2.012$, $J_d \approx 135$ G, $\Delta B_d \approx 29$ G, $w_d \approx 0.65$, $w_w \approx 0.35$}: here, the theoretical EPR spectrum (a thick solid line in C) are deconvoluted into the doublet (a thick solid line in A) and wing (a thick solid line in B) components, each of which is further deconvoluted into four-transition components as indicated. We note that (1) the small asymmetry of the S_3' signal in Fig. 11 is well reproduced by the second order perturbation correction due to the nuclear hyperfine coupling alone; (2) the value of g_2=2.011 is reasonably closer to the free electron g-value (g_e=2.0023) than the g-value of HO_2·, 2.015[38] (see Discussion); and (3) the doublet component arises from ca. 65 % of EPR-susceptible Mn-radical complexes in the S_3' state.

Then, it would be interesting to predict the isotope effect of (DOOD·)$^-$ on the S_3' signal, especially on its doublet component. When proton (I=1/2) is exchanged by deuterium (I=1), the hyperfine coupling constants will be significantly reduced into $a_e \approx a_f \approx 3$ G, as estimated from ≈78/508*20 G[39]. Nevertheless, it was found that the doublet peak intensity of the S_3' signal is increased only slightly (≈11%) by the H/D isotopic replacement, and the other portion will not change almost. Thus, any attempt to detect this small isotope effect on such a weak S_3' signal is required to be especially careful. In addition, it should be noted that the wing component is asymmetrically distributed with an overall width, 950 G, in agreement with the experimental one, 910 G [19].

6. Discussions and conclusions

In the previous sections, we have developed a unified theory of the S_3' signal arising from a variety of modified forms of the S_3 state in Ca^{2+}-depleted, Cl^--depleted, and NH_3-treated samples, and answered to a question why the normal S_3 state is EPR-silent. The theory is based on the most likely assumption that, in both the normal and the modified S_3-states, the Mn cluster can be regarded as a coupled spin system

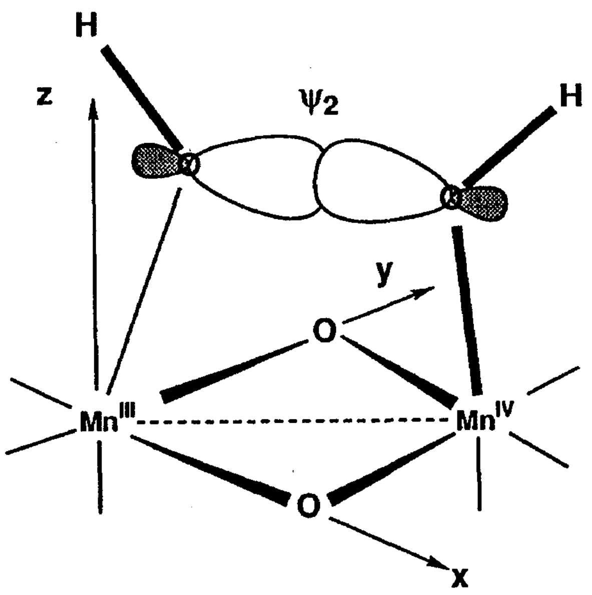

Fig.12 The xyz-coordinate system to describe the anisotropic exchange interaction between a Mn(III) ion in di(μ-oxo) Mn_2(III,IV) subunit and an unpaired electron in the ψ_2-orbital of a bridging radical, (HOOH·)⁻.

consisting of a spin S_1=1/2 Mn-tetramer, which remains essentially the same spin configuration as that in the S_2 state with spin S_1=1/2 [2], and a spin S_2=1/2 radical bound to it as a direct ligand at some appropriate site. We have quantum-mechanically derived an effective spin hamiltonian involving the effective isotropic ($J_{12}\mathbf{S}_1 \cdot \mathbf{S}_2$) and anisotropic ($\mathbf{S}_1 \cdot \mathbf{D}_{12} \cdot \mathbf{S}_2$) interactions as the essential terms that can sensitively reflect the conformational state of the Mn complex and the radical binding state. The necessity of this new theory has arisen from the fact that the S_3' signal consists of two distinguishable components, called "doublet" and "wing", the former exhibiting a near-symmetric split band indicative of a small near-isotropic interaction ($|J_{12}| \approx$ 100-200 G » $|D_{12}|$) [23] and the latter extending over nearly a half range of the dark stable multiline signal indicative of much stronger J_{12} interaction than the nuclear hyperfine splittings, and also from recent flash-induced XANES studies with use of physiologically native PS II membranes in the normal [28] and Ca^{2+}-depleted [29] preparations, indicating that a Mn(III) or Mn(IV) ion or its direct ligand was oxidized upon the $S_2(S_2') \rightarrow S_3(S_3')$ transition, although only the latter possibility, i.e. the oxidation of a ligand at special site(s), can be consistent with the S_3' signal. It was pointed out (Kusunoki et al.[28]) that the 6th coordination site of Mn_a(III) or Mn_b(IV) ion in the di(μ-oxo) bridged Mn_2(III,IV) microsurface can be the most probable candidate, because the XANES K-edge energy could sensitively upshift only when the ligand with the longest bond length is oxidized to be more tightly bound, just as the oxidation of Mn(III) ion to Mn(IV) induces the shortening of a Mn-ligand bond resulting in the upshift of the K-edge energy.

The theory, however, contradicts an earlier report [25] stating that the Mn K-edge XAFS spectrum of a PS II preparation poised in the ≈35% S_2 and ≈65% "S_3" state was the same as that poised in the ≈100% S_2 state: this observation appears to have been utilized as a supporting evidence for an "S_2'-plus-organic radical" model, where the organic radical was not allowed to be a covalent-bonded ligand, because whose oxidation would strengthen and shorten the Mn-ligand bond resulting in an appreciable upshift or modification of the

Mn K-edge XANES spectrum, and was proposed to be a remote His·$^+$ [23], Y_Z·$^+$ [26] and Try·$^+$ [40]. However, it was further pointed out (Kusunoki et al.[28]) that the reported EPR data [25], which were used to evaluate the sample procedures to generate a double turnover of PS II, can be more reasonably re-evaluated as follows, yielding an opposite conclusion of no $S_2 \rightarrow S_3$ advancement due to no reduction of acceptor Fe^{3+} to Fe^{2+} during the illumination at 240 K(step 4): (1) the amplitude of the multiline signal may not be used as a quantitative measure of the S_2-state composition, because it is known that the S_2 state may be inhomogeneous as regards the total spin of the Mn cluster taking a spin S=1/2 or S=5/2 [see a review, Debus[5]], possibly depending upon the temperature and the duration time of the sample treatment [2]; (2) Disappearance of the EPR signals at g=8 and g=5.5 associated with $Q_{400}(Fe^{3+})$ was interpreted[25] as indicating the reduction of Fe^{3+} to Fe^{2+}, but the reduction of Q_A to Q_A^- itself can eliminate these signals owing to the onset of the Q_A^- spin coupled with the Fe^{3+} spin; and (3) An EPR signal at g=1.9, which shows a lineshape significantly different from that observed for Q_A^- coupled with Fe^{2+}, can be more reasonably interpreted[25] as arising from $Q_A^-Fe^{3+}$ than from Q_A^- Fe^{2+}. On the other hand, this theory would explain, of course, the apparent lack of Mn oxidation during the S_2 to S_3 transition in the NMR-proton relaxation enhancement [41] and Y_D^+ EPR spin-lattice relaxation [42] experiments, and, simultaneously, even the flash-induced optical absorption change of the $S_2 \rightarrow S_3$ transition which was observed to be similar to [43], or somewhat different from [44] that of the $S_1 \rightarrow S_2$ transition representing the oxidation of one Mn(III) ion to Mn(IV)(see a review of Debus[5]). This similarlity does not necessarily mean that one Mn(III) ion has been oxidized upon the $S_2 \rightarrow S_3$ transition too. Indeed, the fact that the former spectrum highly coincidentally resembles an absorption spectrum of the intermediate formed from the reaction of OH radical with histidine[24], a very different chemical species, with respect to the peak position, bandwidth, lineshape and amplitude, was utilized as an evidence for that the $S_2' \rightarrow S_3'$ transition corresponds to the oxidation of His[23]. This correspondence, however, seems to be inconsistent in the following points: (i) the absorption spectrum of the suggested [imidazole-OH]· radical complex (Table III in ref 44) consists of only two absorption bands, namely, a main band peaked at 310 nm (4.0 eV) possibly arising from a n→π* transition in the imidazole N3=C4 double bond and a weaker band peaked at 410 nm (3.02 eV) may be ascribable to the C→B transition in OH [45] added to the position C5 [44], and does not contain such a weak shoulder peaked at 350 nm (3.54 eV) as observed in the $S_2' \rightarrow S_3'$ difference spectrum. This discrepancy was first pointed out by Dekker [43], although an absorption spectrum of His· would be in general different from that of [His-OH]·; and (ii) Generally, the higher the spin density on oxygen the higher the g value, because if the atomic shell is less than half full, the atomic spin-orbit coupling constant λ is positive and $g < g_e$, and if the shell is more than half full, $\lambda < 0$ and $g > g_e$. Since an imidazole does not contain oxygen, the g-value of a Hiso radical is expected to be close to g_e. In fact, the [imidazole-OH] radical complex mentioned above takes the value of $g=2.00226 \approx g_e$[44] in agreement with the radical spin primarily localized at the C2 atom. However, King et al.[45] reported significantly higher g values than g_e for some amino acid free radicals formed by oxidation of metmyoglobins, e.g. g=2.009 for His » g_e; and g=2.010 for Gly » {gx=2.0025, gy=2.0038, gz=2.0044} for a crystal of Gly [47], But, in these examples, the unpaired electron is expected to be localized mainly on the peptide carbonyl > C=O. On the other hand, the g value of the radical formed in the S_3' state has been found to be $g_2 \approx 2.011$, in accord with the original estimate[23]. This value, however, seems to be too high to be ascribed to His imidagole as well as the other aromatic amino acids residues, all of which do not contain O atom in the aromatic ring(s).

Therefore, we conclude that such a high g value must have arisen from an O-rich radical formed by the first water oxidation process in the Kok's cycle. The most probable candidate would be an (HOOH·)$^-$ radical bound to the Mn complex that was predicted[48] to appear in the S_3 state as the third bridging ligand between the putative di-μ-oxo bridged Mn(III) and Mn(IV) ions, on the basis of the MO studies on the deprotonation energetics of the water splitting reaction taking place on the catalytic binuclear microsurface, because (i) the $(HOOH\cdot)^-$ radical in the S_3 state can be the only model as an intermediate product obtained by removing two protons and one electron from a water dimer, in accordance with the observed stoichiometry of protons released from the water oxidizing complex per P680 during the S-state cycle, i.e. 1.2:0.2:0.95:1.65 at pH 6.5 for the $S_0 \rightarrow S_1$, $S_1 \rightarrow S_2$, $S_2 \rightarrow S_3$ and $S_3 \rightarrow (S_4) \rightarrow S_0$ transitions, respectively [49]; (ii) this radical can be transiently generated in buffered aqueous solution at the first step in the oxidation of MbIII by H_2O_2 [50]; and (iii) the g value of this radical is expected to be less than that of $OH\cdot$ (≈2.011 [38]) but much larger than g_e, and these conditions are well satisfied by $g_2 \approx 2.011$. If this is the case, the unpaired electron must occupy a σ-type bonding orbital between two O atoms which could be both promoted to provide three approximate $2sp_2$ hybrid orbitals and two lone-pair orbitals if one O atom is coordinated to Mn(III) and the other to Mn(IV) ion in the di(μ-oxo)Mn_2(III,IV) subunit. Moreover, the two O atoms with separation of ca. 1.43 Å are bonded by a doubly-occupied $(2sp_2)\pi$ orbital. Consequently, we suggest that the flash-induced optical absorption spectrum peaked at ≈ 310 nm (main band) and ≈ 350 nm (shoulder band) may be assigned to the $n \rightarrow \sigma^*$ and $(2sp_2)\pi \rightarrow \sigma$ transitions in the O-O bond, respectively. In addition, it is important to note that the Mn(IV)-O bond must be stronger than the Mn(III)-O, giving rise to such an asymmetric bridge ligation as schematically depicted in Fig.4A , which in turn leads to a small $(2J_{a2} - J_{b2})$ in eq 37 due to a large body of cancellation between the exchange interactions, $2J_{a2}$ and J_{b2}.

Indeed, we have shown that only this $(HOOH\cdot)^-$ radical can reasonably explain the doublet component of the S_3' signal only when it forms a similar asymmetric third bridging ligand between the di-μ-oxo bridged Mn(III) and Mn(IV) ions on the opposite side of the other pair of Mn(IV) ions in the $S_1=1/2$ Mn-tetramer, which would take a distorted structure (model **A2c** in Table 1), and whose spin wave function could be approximately expanded as eq 5 with $-\theta_0 \approx 63\text{-}65°$. Namely, only this special form of the Mn-radical complex has been shown to simultaneously satisfy the following three conditions for the near-symmetric and hence near-isotropic S_3' signal: (i) an extremely small effective exchange interaction, i.e. $|J_{12}| \approx 100\text{-}200$ G; and (ii) much smaller magnetic dipolar interactions, i.e. $|D_{12}| << |J_{12}|$ and $|E_{12}| << |J_{12}|$, when the phase angle θ_0 happens to be shifted into a narrow range within ±1° around the magic phase angle $\theta_B{}^A$ (condition (i)) which must lie slightly (2°-5°) above -60° (conditions (ii)). For this hapening to take place with an apprecible probability (roughly estimated as $\approx 0.23*w_d \approx 0.16$ according to Gilchrist et al.[22]), there must exist an inhomogeneous distribution of J_{12} at least in the S_3' state. In fact , the wing component of the S_3' signal has been shown to arise from different Mn-radical complexes having much larger J_{12} than 100-200 G, although the percentage of these complexes seems to be only ≈ 8 % (≈ 23%*w_w). Furthermore, the majority of Mn-radical complexes (≈ 77 %) are known to be EPR-silent, and we have proposed this is because these complexes carry no net magnetic moments owing to $J_{12} \gg k_BT$ (the singlet ground state). Thus, we have pointed out that the S_3' state is evidently inhomogeneous, suggesting that the Ca^{2+} cofactor is bound near the Mn complex, and its depletion would result in a variety of relaxed conformational states of the Mn cluster. Recently, Yachandra et al.[4] proposed, based on EXAFS measurements, that a Ca^{2+} ion is located approx. 3.3 Å from Mn, supporting our suggestion.

On the other hand, a dimer-of-dimers model proposed on the basis of EXAFS data[4] must uniquely correspond to the present model B as depicted in Fig. 4B, whose spin wave function can be well described by eq 5 with θ_0 being always near 0°. We have shown that only the model **Ba** can be consistent with the near-symmetric and hence near-isotropic split EPR signal in a vanishingly small range of θ_0 around -1.05° (see Table 1). But, such a small θ_0 has been shown in Fig. 6b to cause an enhanced hyperfine structure in the wing regions against the experimental observation. Hence, it is concluded that if the doublet spectrum in the oriented Ca^{2+}-depleted PS II is observed to be really isotropic both in position and in intensity, the Mn-radical complex must belong to model **A2c**, but if it is so only in position, the complex can be either model **A** or **B** as far as the spectral lineshape is concerned, because then the magic angle effect described in Section 5.3 must have happened to take place.

Appendix A Matrix elements of projection operators $\{P_i = \mathbf{S}_i \cdot \mathbf{S}_1/[S_1(S_1+1)];\ i=\text{a-d}\}$ in the $[S_{ab}S_{cd}S_1]$ representation

$$\langle S_{ab}S_{cd}S_1M|P_a|S'_{ab}S_{cd}S_1M\rangle = \left\{\frac{1}{2}+\frac{S_{ab}(S_{ab}+1)-S_{cd}(S_{cd}+1)}{2S_1(S_1+1)}\right\} \cdot\left\{\frac{1}{2}+\frac{S_a(S_a+1)-S_b(S_b+1)}{2S_{ab}(S_{ab}+1)}\right\}\delta_{S_{ab}S'_{ab}} + \frac{[(S_1+S_{ab}+S_{cd}+2)(-S_1+S_{ab}+S_{cd}+1)(S_1-S_{ab}+S_{cd})]^{1/2}}{2S_1(S_1+1)(S_{ab}+1)[(2S_{ab}+1)(2S_{ab}+3)]^{1/2}} \cdot[(S_a+S_b+S_{ab}+2)(S_a-S_b+S_{ab}+1)(-S_a+S_b+S_{ab}+1)(S_a+S_b-S_{ab})]^{1/2}\delta_{S'_{ab}S_{ab}+1}, \tag{A1}$$

$$\langle S_{ab}S_{cd}S_1M|P_b|S'_{ab}S_{cd}S_1M\rangle = \left\{\frac{1}{2}+\frac{S_{ab}(S_{ab}+1)-S_{cd}(S_{cd}+1)}{2S_1(S_1+1)}\right\} \cdot\left\{\frac{1}{2}+\frac{S_b(S_b+1)-S_a(S_a+1)}{2S_{ab}(S_{ab}+1)}\right\}\delta_{S_{ab}S'_{ab}} - \frac{[(S_1+S_{ab}+S_{cd}+2)(-S_1+S_{ab}+S_{cd}+1)(S_1-S_{ab}+S_{cd})]^{1/2}}{2S_1(S_1+1)(S_{ab}+1)[(2S_{ab}+1)(2S_{ab}+3)]^{1/2}} \cdot[(S_a+S_b+S_{ab}+2)(S_a-S_b+S_{ab}+1)(-S_a+S_b+S_{ab}+1)(S_a+S_b-S_{ab})]^{1/2}\delta_{S'_{ab}S_{ab}+1}, \tag{A2}$$

$$\langle S_{ab}S_{cd}S_1M|P_c|S_{ab}S'_{cd}S_1M\rangle = \left\{\frac{1}{2}+\frac{S_{cd}(S_{cd}+1)-S_{ab}(S_{ab}+1)}{2S_1(S_1+1)}\right\} \cdot\left\{\frac{1}{2}+\frac{S_c(S_c+1)-S_d(S_d+1)}{2S_{cd}(S_{cd}+1)}\right\}\delta_{S_{cd}S'_{cd}} + \frac{[(S_1+S_{ab}+S_{cd}+2)(-S_1+S_{ab}+S_{cd}+1)(S_1-S_{ab}+S_{cd})]^{1/2}}{2S_1(S_1+1)(S_{cd}+1)[(2S_{cd}+1)(2S_{cd}+3)]^{1/2}} \cdot[(S_c+S_d+S_{cd}+2)(S_c-S_d+S_{cd}+1)(-S_c+S_d+S_{cd}+1)(S_c+S_d-S_{cd})]^{1/2}\delta_{S'_{cd}S_{cd}+1}, \tag{A3}$$

and

$$\langle S_{ab}S_{cd}S_1M|P_d|S_{ab}S'_{cd}S_1M\rangle = \left\{\frac{1}{2}+\frac{S_{cd}(S_{cd}+1)-S_{ab}(S_{ab}+1)}{2S_1(S_1+1)}\right\} \cdot\left\{\frac{1}{2}+\frac{S_d(S_d+1)-S_c(S_c+1)}{2S_{cd}(S_{cd}+1)}\right\}\delta_{S_{cd}S'_{cd}} - \frac{[(S_1+S_{ab}+S_{cd}+2)(-S_1+S_{ab}+S_{cd}+1)(S_1-S_{ab}+S_{cd})]^{1/2}}{2S_1(S_1+1)(S_{cd}+1)[(2S_{cd}+1)(2S_{cd}+3)]^{1/2}} \cdot[(S_c+S_d+S_{cd}+2)(S_c-S_d+S_{cd}+1)(-S_c+S_d+S_{cd}+1)(S_c+S_d-S_{cd})]^{1/2}\delta_{S'_{cd}S_{cd}+1}. \tag{A4}$$

Appendix B Anisotropic exchange or pseudo-dipolar interaction between a Mn(III) ion and a ligand radical

We discuss the magnetic interactions between a Mn(III) ion in di(μ-oxo)Mn_2(III, IV) dimer and an unpaired electron in the third bridging ligand such as $(HOOH\cdot)^-$, by using the xyz coordinate system defined in Fig. 12. The interaction hamiltonian H_{int} between the d-electrons and the σ-electron in a φ_2-orbital consists of a direct Coulomb and some superexchange(K) interactions:

$$H_{int} = \sum_{k=1}^{4} h_{int} \equiv \sum_{k=1}^{4}\left\{\frac{e^2}{|\mathbf{r}_k-\mathbf{r}_2|}+K(\mathbf{r}_k,\mathbf{r}_2)\right\}. \tag{B1}$$

In the ^5A ground state of the Mn(III) ion, the occupied d-orbitals may be assumed to be {d(xy), d(yz), d(zx), d($3z^2$-r^2)}, which are defined as $\{d_k;\ k=1, 2, 3, 4\}$ in this order, owing to the Jahn-Teller elongation along the z-direction. The energy difference between ferromagnetic and antiferromagnetic states described by Slater determinants, $|d(xy)d(yz)d(zx)d(3z^2-r^2)\Psi_2|$ and

$|d(xy)d(yz)d(3z^2-r^2)\Psi_2|$, respectively, defines the isotropic exchange integral J_{a2} as

$$J_{a2} = \frac{2}{2S_a+1}\{\int d\tau |d(yz)d(zx)d(xy)d(3z^2-r^2)\psi_2|^* H_{int} \cdot |d(yz)d(zx)d(xy)d(3z^2-r^2)\psi_2| - \int d\tau |d(yz)d(zx)d(xy)d(3z^2-r^2)\overline{\psi_2}|^* H_{int} \cdot |d(yz)d(zx)d(xy)d(3z^2-r^2)\overline{\psi_2}|\} = -\frac{2}{2S_a+1}\sum_{k=1}^{4}\langle d_k\psi_2|h_{int}|\psi_2 d_k\rangle, \tag{B2}$$

giving rise to the effective spin hamiltonian $J_{a2}\mathbf{S}_a\cdot\mathbf{S}_2$. In this expression, the Coulomb potential terms represent the ferromagnetic direct exchange and the K terms the antiferromagnetic exchange. These exchange interactions may cancel to each other, resulting in a rather weak exchange interaction, possibly because the closed-shell di-μ-oxo ions can play an intervening role on the $\approx 90°$ indirect exchange.

On the other hand, the effect of spin-orbit interaction H_{LSa} in $Mn_a(III)$ ion on the anisotropic exchange interaction can be well described by the lowest-order perturbation process in which the spin-dependent interaction is involved, as given by [32]

$$H'_{exch} = \sum_{e,e'}\frac{(\psi_{ag}|H_{LSa}|\psi_{ae})(\psi_{ae}\psi_2|H_{int}|\psi_{ae'}\psi_2)(\psi_{ae'}|H_{LSa}|\psi_{ag})}{\Delta E_{eg}\Delta E_{e'g}} \tag{B3}$$

where the other minor processes have been neglected, Ψ_{ag} in $|\Psi_{ag}\Psi_2)$ represents the d-orbital part of the Slater determinant of the ground state, and Ψ_{ae} in $|\Psi_{ae}\Psi_2)$ does that of an excited state. H_{LSa} may be approximated by $\lambda_a\mathbf{L}_a\cdot\mathbf{S}_a$, which connects the ground singlet (^5S) and the excited triplet (^5P) states of Mn(III) ion whose wave functions are given by

$$\psi_{aex} = [d(yz), d(xy), d(3x^2-r^2), d(z^2-y^2)],$$
$$\psi_{aey} = [d(xy), d(yz), d(3y^2-r^2), d(z^2-x^2)],$$

and

$$\psi_{aez} = [d(yz), d(zx), d(3z^2-r^2), d(x^2-y^2)]. \tag{B3}$$

The non-vanishing matrix elements of $\mathbf{L}_a$ between the ^5S and ^5P states are found to be

$$(\psi_{aex}\psi_2|L_{ax}|\psi_{ag}\psi_2) = (\psi_{aey}\psi_2|L_{ay}|\psi_{ag}\psi_2) = (\psi_{aez}\psi_2|L_{az}|\psi_{ag}\psi_2) = -2i. \tag{B4}$$

The matrix elements of H_{int} in this triplet may be approximated by $J_x\mathbf{S}_a\cdot\mathbf{S}_2$, $J_y\mathbf{S}_a\cdot\mathbf{S}_2$ and $J_z\mathbf{S}_a\cdot\mathbf{S}_2$, where

$$J_x = J_{a2} + \frac{2}{2S_a+1}\left[\begin{array}{c}\langle d(x^2-y^2)\psi_2|h_{int}|\psi_2 d(x^2-y^2)\rangle \\ -\langle d(yz)\psi_2|h_{int}|\psi_2 d(yz)\rangle\end{array}\right],$$

$$J_y = J_{a2} + \frac{2}{2S_a+1}\left[\begin{array}{c}\langle d(x^2-y^2)\psi_2|h_{int}|\psi_2 d(x^2-y^2)\rangle \\ -\langle d(zx)\psi_2|h_{int}|\psi_2 d(zx)\rangle\end{array}\right],$$

and

$$J_z = J_{a2} + \frac{2}{2S_a+1}\left[\begin{array}{c}\langle d(x^2-y^2)\psi_2|h_{int}|\psi_2 d(x^2-y^2)\rangle \\ -\langle d(xy)\psi_2|h_{int}|\psi_2 d(xy)\rangle\end{array}\right]. \tag{B5}$$

Since $\Delta E_{eg} \approx \Delta E = 10Dq$ (the conventional crystalline field parameter), we get from eqs B2, B4 and B5

$$H'_{exch} = \left(\frac{2\lambda_a}{\Delta E}\right)^2\left[\begin{array}{c}J_xS_{ax}(\mathbf{S}_a\cdot\mathbf{S}_2)S_{ax} + J_yS_{ay}(\mathbf{S}_a\cdot\mathbf{S}_2)S_{ay} \\ +J_zS_{az}(\mathbf{S}_a\cdot\mathbf{S}_2)S_{az}\end{array}\right]. \tag{B6}$$

Eq B6 can not be further simplified because of S_a=2, which is a different situation from the cases of Ni(II) with S=1 and Cu(II) with S=1/2. But, we do not need H'_{exch} itself but do its effective spin hamiltonian H'_{exch}* in the S_1=1/2 ground state of Mn_4(III,IV,IV,IV) tetramer described by the wave function $\Psi_1(1/2,M)$ of eq 5. H'_{exch}* can be obtained by the vector projection method based on the Wigner-Eckart theorem [31]:

$$H'^{*}_{exch} = \left(\frac{2\lambda_a}{\Delta E}\right)^2 \begin{bmatrix} J_x\{(C_1 - C_2)S_{1x}{}^3S_{2x} + C_2S_{1x}(S_1\cdot S_2)S_{1x}\} \\ +J_y\{(C_1 - C_2)S_{1y}{}^3S_{2y} + C_2S_{1y}(S_1\cdot S_2)S_{1y}\} \\ +J_z\{(C_1 - C_2)S_{1z}{}^3S_{2z} + C_2S_{1z}(S_1\cdot S_2)S_{1z}\} \end{bmatrix}, \tag{B7}$$

with

$$C_1 = \frac{\langle\psi_1(\frac{1}{2}m)\|S_{ai}{}^3\|\psi_1(\frac{1}{2}m)\rangle}{\langle\psi_1(\frac{1}{2}m)\|S_{1i}{}^3\|\psi_1(\frac{1}{2}m)\rangle} = \frac{68}{5}P_a(\theta_0); \text{for } i = x,y,z \tag{B8}$$

and

$$C_2 = \frac{\langle\psi_1(\frac{1}{2}m)\|S_{ai}S_{aj}S_{ai}\|\psi_1(\frac{1}{2}m)\rangle}{\langle\psi_1(\frac{1}{2}m)\|S_{1i}S_{1j}S_{1i}\|\psi_1(\frac{1}{2}m)\rangle} = -\frac{64}{5}P_a(\theta_0); \text{for } i,j = x,y,z (i \neq j). \tag{B9}$$

Eq B7 can be simplified by use of the relations (S_1=1/2): $S_{1i}{}^3 = S_{1i}/4$; i=x,y,z and $S_{1i}S_{1j}S_{1i} = -S_{1j}/4$; i, j=x,y,z ($i \neq j$). It is now straightforward to show that an anisotropic part in $H'_{exch}{}^*$ yields the pseudo-dipolar effective spin hamiltonian given by

$$H_{pd} = (E_{pd} - \frac{1}{3}D_{pd})S_{1x}S_{2x} + (E_{pd} + \frac{1}{3}D_{pd})S_{1x}S_{2x} + \frac{2}{3}D_{pd}S_{1z}S_{2z}, \tag{B10}$$

with

$$D_{pd} = \left(\frac{\lambda_a}{\Delta E}\right)^2 \Delta J_D P_a(\theta_0), \Delta J_D = -\frac{2}{5}(J_x + J_y - 2J_z) \tag{B11}$$

and

$$E_{pd} = \left(\frac{\lambda_a}{\Delta E}\right)^2 \Delta J_E P_a(\theta_0), \Delta J_E = \frac{2}{5}(J_x - J_y). \tag{B12}$$

From eq B5, we can estimate the axial and rhombic exchange parts, ΔJ_D of eq B11 and ΔJ_E of eq B12, respectively, as

$$\begin{aligned} \Delta J_D &= \frac{4}{25}\{\langle d(yz)\psi_2|h_{int}|\psi_2 d(yz)\rangle \\ &\quad +\langle d(xz)\psi_2|h_{int}|\psi_2 d(xz)\rangle \\ &\quad -2\langle d(xy)\psi_2|h_{int}|\psi_2 d(xy)\rangle\} \\ &\approx \frac{8}{25}\langle d(yz)\psi_2|h_{int}|\psi_2 d(yz)\rangle \end{aligned} \tag{B13}$$

and

$$\begin{aligned} \Delta J_E &= \frac{4}{25}\{\langle d(xz)\psi_2|h_{int}|\psi_2 d(xz)\rangle \\ &\quad - \langle d(yz)\psi_2|h_{int}|\psi_2 d(yz)\rangle\} \approx 0. \end{aligned} \tag{B14}$$

The value of $\lambda_a/\Delta E$ can be estimated from the observed g_z-value ($g_z \approx 1.963$) according to the approximate relation[51], $\lambda_a/\Delta E \approx (2.0023 - g_z)/8 \approx 0.005$. Therefore, the pseudo-dipolar term may be neglected in the present problem.

References

[1] B. Kok, B. Forbush and M. MacGloin, Photochem. Photobiol. 11 (1970) 457. P. Joliot, G. Barbiéri and R. Chaboud, Photochem. Photobiol. 10 (1969) 309.

[2] M. Kusunoki, Chem. Phys. Letters 197 (1992) 108.

[3] J. Bonvoisin, G. Blondin, J.-J. Girerd and J.-L. Zimmermann, Biophys. J. 61 (1992) 1076.

[4] V.K. Yachandra, V.J. DeRose, M.J. Latimer, I. Mukerji, K. Sauer and M.P. Klein, Science **1993**, 260 (1993) 675.

[5] R.J. Debus, Biochim. Biophys. Acta 1102 (1992) 269. Ö. Hansson, T. Wydrzynski, Photosynth. Res. 23 (1990) 131. G. Renger and T. Wydrzynski, Biol. Metals 4 (1991) 73. A.W. Rutherford, A. Boussac and J.-L. Zimmermann, New J. Chem. 15 (1991) 491.

[6] G.C. Dismukes and Y.Siderer, Proc. Natl. Acad. Sci. USA 78 (1981) 274.

[7] A. Boussac, J.-L. Zimmermann and A.W. Rutherford, Biochemistry 28 (1989) 8984.

[8] M. Sivaraja, J. Tso and D.C. Dismukes, Biochemistry 28 (1989) 9459.

[9] T. Ono and Y. Inoue, Biochim. Biophys. Acta 1015 (1990) 373.

[10] W.F. Beck and G.W. Brudvig, Biochemistry 25 (1989) 6479.

[11] M. Kusunoki, In: Research in Photosynthesis, Vol. 2, ed. N. Murata (Kluwer Academic Publishers, Dordrecht, 1992) p 297.

[12] M. Kusunoki, T. Ono, M. Suzuki, T. Noguchi, A. Uehara, T. Matsushita, H. Oyanagi and Y. Inoue, In: Research in Photosynthesis, Vol. 2, ed. N. Murata (Kluwer Academic Publishers, Dordrecht, 1992) p 293.

[13] J.L. Casey and K. Sauer, Biochim Biophys Acta 767 (1984) 21.

[14] J.-L. Zimmermann and A.W. Rutherford, Biochim. Biophys. Acta 767 (1984) 160.

[15] D.H. Kim, R.D. Britt, M.P. Klein and K. Sauer, Biochemistry 31 (1992) 541.

[16] A. Haddy, W.R. Dunham, R.H. Sands and R. Aasa, Biochemistry 1099 (1992) 25.

[17] Ö. Hansson, R. Aasa and T. Vänngård, Biophys. J. 51 (1987) 825.

[18] S.L. Dexheimer and M.P. Klein, J. Am. Chem. Soc. 114 (1992) 2821.

[19] L.-E. Andréasson and K. Lidberg, Biochim. Biophys. Acta 1100 (1992) 177.

[20] D.J. McLachlan, N.H.A. Nugent and M.C.W. Evans, In: Research in Photosynthesis, Vol. 2, ed. N. Murata (Kluwer Academic Publishers, Dordrecht, 1992) p 373.

[21] J. Tso, M. Sivaraja, J.S. Philo and G.C. Dismukes, Biochemistry **1991**, 30 (1991) 4740.

[22] M.L. Gilchrist, G.A. Lorigan and R.D. Britt, In: Research in Photosynthesis, Vol. 2, ed. N. Murata (Kluwer Academic Publishers, Dordrecht, 1992) p 317.

[23] A. Boussac, J.-L. Zimmermann and A.W. Rutherford, FEBS Letters 277 (1990) 69. A. Boussac, J.-L. Zimmermann, A.W. Rutherford and J. Lavergne, Nature 347 (1990) 303.

[24] P.S. Rao, M. Sinic and E. Hayon, J. Phys. Chem. 79 (1975) 1260.

[25] R.D. Guiles, V.K. Yachandra, A.E. McDermott, J.L. Cole, S.L. Dexheimer, R.D. Britt, K. Sauer and M.P. Klein, Biochemistry 29 (1990) 486. R.D. Guiles, J.-L. Zimmermann, A.E. McDermott, V.K. Yachandra, J.L. Cole, S.L. Dexheimer, D. Britt, K. Wieghardt, U. Bossek, K. Sauer and M.P. Klein, Biochemistry 29 (1990) 471.

[26] B.J. Hallahan, J.H.A. Nugent, J.T. Warden, M.C.W. Evans, Biochemistry 31 (1992) 4562.

[27] Boussac, A; Rutherford, A. W. *Biochemistry*, **1992**, 31, 7441-7445.

[28] T. Ono, T. Noguchi, Y. Inoue, M. Kusunoki, T. Matsushita, H. Oyanagi, Science 258 (1992)1335. M. Kusunoki, T. Ono, T. Noguchi, Y. Inoue and H. Oyanagi, Photosynthesis Reserach 38 (1993) 331.

[29] T. Ono, M. Kusunoki, T. Matsushita, H. Oyanagi and Y. Inoue, Biochemistry 30 (1991) 6836. T. Ono, T. Noguchi, Y. Inoue, M. Kusunoki, H. Yamaguchi and H. Oyanagi, FEBS Letters 330 (1993) 28.

[30] R.G. Evelo, S. Styring, A.W. Rutherford and A.J. Hoff, Biochim. Biophys. Acta 973 (1989) 428.

[31] D.A. Varshalovich, A.N. Moskaev and V.K. Khersonskii, Quantum theory of angular momentum (World Scientific, Singapore, 1988) p 1.

[32] J. Kanamori, In: Magnetism , Vol I, eds. G.T. Rado and H. Suhl (Academic Press, New York, 1963) p 127.

[33] J. Máthé, C. J. Schinkel and W. A. van Amstel, Chem. Phys. Letters 33 (1975) 528.

[34] N. Auger, J.-J. Girerd, M. Corbella, A. Gleizes and J.-L. Zimmermann, J. Am. Chem. Soc. 112 (1990) 448.

[35] P.W. Anderson and P.R. Weiss, Reviews of Modern Physics. 25 (1963) 269.

[36] M. Andon and A. Bino, Structure and Bonding 65 (1987) 1.

[37] H. M. Swarts, J. R. Bolton and D. C. Borg, Biological Application of Electron Spin Resonance (Wiley Interscience, New York, 1972) p. 463.

[38] R. Livington and H. Zeldes, J. Chem. Phys. 44 (1966) 1245.

[39] P. W. Atkins, M. C. R. Symons, The Structure of Inorganic Radicals (Elsevier, New York, 1967) p. 21.

[40] J. Lavergne, Photochem. Photobiol. 1060 (1991) 175.

[41] R. R. Sharp, In: Manganese Redox Enzymes , ed. V.L. Pecoraro (VCH, New York, 1992) p. 177.

[42] S.A. Styring and A.W. Rutherford, Biochemistry 27 (1988) 4915.

[43] J.P. Dekker, In: Manganese Redox Enzymes , ed. V.L. Pecoraro (VCH, New York, 1992) p. 85.

[44] A. Samuni and P. Neta, J. Phys. Chem. 77 (1973) 1629.

[45] N. K. King and M. E. Windfield, J. Biol. Chem.238 (1963) 1520.

[46] C. Hoganson and G. T. Babcock, Biochemistry 27 (1988) 5848.
[47] H.C. Box, H.G. Freund and E.E. Budzinski, J. Am. Chem. Soc. 88 (1966) 658.
[48] M. Kusunoki, In: Progress in Photosynthesis Research , Vol I, ed. J. Biggins (Martinus Nijhoff Publishers, Dordrecht, 1987) p. 729.
[49] F. Rappaport and J. Lavergne, Biochemistry 30 (1991) 10004.
[50] N. K. King and M. E. Windfield, Biochim. Biophys. Acta 133 (1967) 65.
[51] A. Abragam and B. Bleaney, Electron Paramagnetic Resonance of Transition Ions (Dover Publications, New York, 1986) p. 434.